

DISSERTATION

ARTIFICIAL GROUND WATER RECHARGE WITH CAPILLARITY

Submitted by

Nestor Ortiz

In partial fulfillment of the requirements

for the Degree of Doctor of Philosophy

Colorado State University

Fort Collins, Colorado

Spring, 1977

COLORADO STATE UNIVERSITY

May 5 19 77

WE HEREBY RECOMMEND THAT THE DISSERTATION PREPARED UNDER
OUR SUPERVISION BY Nestor Ortiz

ENTITLED ARTIFICIAL GROUND WATER RECHARGE WITH CAPILLARITY

BE ACCEPTED AS FULFILLING THIS PART OF THE REQUIREMENTS FOR THE DEGREE
OF DOCTOR OF PHILOSOPHY.

Committee on Graduate Work

Robert L. Longenecker
Daniel H. Serrada
Adviser

David W. Zachman
Eric Thompson
D.B. McWhorter

Head of Department

ABSTRACT

The effect of the capillary region on the transient response of the water table to recharge was studied. A two-dimensional model was developed to simulate growth of groundwater mounds when flow and storage in the capillary region are significant. The contribution from the capillary region was described analytically in terms of measurable soil properties and recharge rate.

A series of laboratory experiments, simulating the spreading of groundwater mounds due to steady recharge from a narrow strip, was conducted. The adequacy of the numerical model in predicting mound height was verified by comparing its solution with the results obtained from the physical model.

The numerical model was used to generate a series of solutions to determine the effect of bubbling pressure head, pore-size distribution index, initial saturated depth, depth to water table and recharge rate on predicted mound height. The results indicate that the effect of capillarity significantly influences the development of groundwater mounds. For practical cases where the initial saturated thickness is large, the influence of capillary storage is much more important than capillary flow. Directly beneath the recharge area, in-transit water has a significantly greater effect on capillary storage than the contributions from the static moisture content profile. The effect of the

capillary region increases for decreasing pore-size distribution index, decreasing initial saturated depth and increasing recharge rate. Previously available solutions underestimate the growth of groundwater mounds by as much as 56 percent at least for the practical case analyzed.

Nestor Ortiz
Civil Engineering Department
Colorado State University
Fort Collins, Colorado 80523
Spring, 1977

ACKNOWLEDGEMENTS

The author wishes to express his appreciation to the members of his graduate committee: Prof. R. A. Longenbaugh, adviser, Dr. D. B. McWhorter, Dr. E. G. Thompson, Dr. D. W. Zachmann and especially to Dr. D. K. Sunada, co-adviser, and Dr. H. R. Duke for their guidance and suggestions throughout this study.

Special thanks are due to Mr. J. A. Brookman for his assistance in setting up the experimental apparatus and to Mrs. Diane English for typing the initial draft and final manuscript.

Sincere appreciation to the Instituto Nacional de Obras Sanitarias, Republic of Venezuela, for financial support and to Colorado State University Experiment Station Project 1110 for partial support.

TABLE OF CONTENTS

<u>Chapter</u>	<u>Page</u>
Abstract	iii
Acknowledgements	v
List of Tables	viii
List of Figures	ix
List of Symbols	xi
I INTRODUCTION	1
II REVIEW OF LITERATURE	3
2.1 State of Art in Groundwater Recharge	3
2.2 Parameters Describing Capillary Properties	4
2.3 Treatment of the Capillary Region	7
III DEVELOPMENT OF THE PROBLEM	11
3.1 Equivalent Permeable Height	14
3.2 Equivalent Saturated Height	16
3.3 Development of Expression for the Specific Yield	19
IV NUMERICAL SOLUTION	22
4.1 The Finite Difference Equations	22
4.2 Procedure for Analysis	25
V VERIFICATION OF NUMERICAL MODEL	28
5.1 Comparison With Analytical Procedure	28
5.2 Verification With Physical Model	30
5.2.1 Description of the physical model	30
5.2.2 Fluid and media	33
5.2.3 Determination of media properties	35
5.2.4 Measurement of hydraulic head in the model	37
5.2.5 Recharge experiment	38

TABLE OF CONTENTS (Cont'd)

<u>Chapter</u>	<u>Page</u>
5.2.6 Comparison with physical model	39
VI RESULTS AND DISCUSSION	46
6.1 Influence of the Capillary Region on Analytical Solutions	46
6.2 Mound Growth Evaluation	51
6.2.1 Influence of capillary storage and capillary flow	51
6.2.2 Influence of bubbling pressure head	57
6.2.3 Influence of pore-size distribution index	59
6.2.4 Influence of initial saturated depth	59
6.2.5 Influence of depth to water table	62
6.2.6 Influence of recharge rate	62
VII SUMMARY AND CONCLUSIONS	65
REFERENCES	67
APPENDIX A - DESCRIPTION OF PROGRAM RECAP1	71
A-1 Boundary and Initial Condition	71
A-2 Selection of Time Increment	71
A-3 Description of Subprograms	72
A-4 Program Listing	75
APPENDIX B - RESULTS FROM EXPERIMENTAL TESTS	85

LIST OF TABLES

<u>Table</u>	<u>Page</u>
5-1 Properties of Porous Material	37
B-1 Mound Growth Results From Experimental Tests: Glass Beads .	85
B-2 Mound Growth Results From Experimental Tests: Glass Beads .	86
B-3 Mound Growth Results From Experimental Tests: Glass Beads .	87
B-4 Mound Growth Results From Experimental Tests: Ottawa Sand .	88

LIST OF FIGURES

<u>Figure</u>	<u>Page</u>
3-1 Diagrammatic representation of a groundwater mound beneath a spreading basin	12
3-2 Capillary pressure profile in a soil a) in static equilibrium with a water table, b) with a steady downward flux .	18
4-1 Finite difference grid and its physical significance . . .	24
4-2 Sequence of computational events	27
5-1 Comparison of mound shape between numerical model and Glover's solution - no capillary effects	31
5-2 Drawing of experimental model	32
5-3 End box and constant head tank	34
5-4 Relative conductivity as a function of capillary pressure head	36
5-5 View of piezometer	38
5-6 Comparison of mound shape between numerical model and experimental results	40
5-7 Comparison of mound shape between numerical model and experimental results	41
5-8 Comparison of mound shape between numerical model and experimental results	42
5-9 Comparison of mound shape between numerical model and experimental results	43
6-1 Comparison of mound shape between experimental and numerical model and Glover's solution	47
6-2 Comparison of central mound height between numerical model and Glover's solution	49

LIST OF FIGURES (Cond'd)

<u>Figure</u>	<u>Page</u>
6-3 Comparison of mound height between numerical model and Glover's solution at 150 meters from edge of recharge area.	50
6-4 Comparison of the relative importance of capillary flow and capillary storage on central mound height	52
6-5 Comparison of the relative importance of capillary storage and capillary flow at 150 meters from edge of recharge area	53
6-6 Comparison of the relative importance of capillary storage and capillary flow on central mound height	55
6-7 Comparison of the relative importance of capillary storage and capillary flow at 125 cm from edge of recharge area . .	56
6-8 Effect of bubbling pressure head on the rate of growth of mound	58
6-9 Effect of pore-size distribution index on the rate of growth of mound	60
6-10 Effect of initial saturated thickness on rate of growth of mound	61
6-11 Effect of depth to water table on rate of growth of mound .	63
6-12 Effect of scaled flux rate on central mound height	64

LIST OF SYMBOLS

<u>Symbol</u>	<u>Definition</u>	<u>Dimension</u>
a	Constant in Gardner's equation for capillary conductivity	none
b	Constant in Gardner's equation for capillary conductivity	none
D	Depth from ground surface to the impermeable base	L
F	Force	F
g	Acceleration due to gravity	LT^{-2}
h	Water table elevation referred to impermeable lower boundary	L
H	Piezometric head	L
H'	Distance from the water table to soil surface	L
HF	Available depth for horizontal flow	L
H_k	Equivalent permeable height	L
H_0	Initial saturated thickness	L
H_s	Equivalent saturated height	L
$H_{k.}$	Scaled permeable height - $H_k/(P_b/\rho g)$	none
$H_{s.}$	Scaled saturated height - $H_s/(P_b/\rho g)$	none
h_c	Water table elevation at midpoint between drains	L
h_d	Water table elevation at drain outlet	L
i	An infiltration rate	LT^{-1}
i	Row number of grid	none
j	Column number of grid	none
K	Saturated hydraulic conductivity	LT^{-1}
K_e	Capillary conductivity	LT^{-1}

LIST OF SYMBOLS (Cont'd)

<u>Symbol</u>	<u>Definition</u>	<u>Dimension</u>
k	Intrinsic permeability at saturation	L^2
k_e	Effective permeability	L^2
K_r	Relative conductivity - K_e/K	none
k_r	Relative permeability - k_e/k	none
L	Length	L
L	Drain spacing	L
n	Constant in Gardner's equation	none
P	Fluid pressure	FL^{-2}
P.	Scaled capillary pressure - P_c/P_b	none
P_b	Bubbling pressure	FL^{-2}
P_c	Capillary pressure	FL^{-2}
$P_{s.}$	Scaled capillary pressure at the soil surface	none
q	Volume flux rate	LT^{-1}
Q	Net groundwater withdrawal	L^3T^{-1}
q.	Scaled flux rate - q/K	none
Q_d	Total drain outflow	L^2T^{-1}
S	Saturation	none
S_e	Effective saturation - $(S-S_r)/(1-S_r)$	none
S_r	Residual saturation - the saturation at which K_e is essentially zero	none
S_y	Specific yield	none
T	Time	T
t	Time	T
W	Width of recharge strip	L
x	Horizontal space variable - x-direction	L

LIST OF SYMBOLS (Cont'd)

<u>Symbol</u>	<u>Definition</u>	<u>Dimension</u>
y	Horizontal space variable - y-direction	L
z	Elevation above the water table	L
z.	Scaled elevation above the water table	none
z'	Elevation at which the capillary pressure equals the bubbling pressure	L
z''	Elevation at which the effective conductivity approaches the flux in magnitude	L
z!	Scaled elevation at which the capillary pressure equals the bubbling pressure - $z'/(P_b/\rho g)$	none
z''	Scaled elevation at which the effective conductivity approaches the flux in magnitude - $z''/(P_b/\rho g)$	none
∂	Partial differential operator	none
α	A constant for a given aquifer which defines the rapidity with which a transient change will take place - KH_o/ϕ_e	L^2T^{-1}
η	Exponent in the equation $K_r = (P_b/P_c)^\eta$	none
θ	Volumetric water content	none
θ_r	Residual water content	none
λ	Pore-size distribution index	none
μ	Dynamic viscosity	$FL^{-2}T$
ρ	Fluid density	FT^2L^{-4}
ρ_b	Bulk density	FT^2L^{-4}
ρ_s	Particle density	FT^2L^{-4}

LIST OF SYMBOLS (Cont'd)

<u>Symbol</u>	<u>Definition</u>	<u>Dimension</u>
ϕ	Total porosity	none
ϕ_e	Drainable porosity - $(1-S_r)\phi$	none

CHAPTER I

INTRODUCTION

The Recharge Phenomena

The demand for water by an increasing population of the world has placed greater emphasis on the exploitation and utilization of groundwater resources for irrigation, industrial and domestic water supply. In many aquifers, present groundwater withdrawals exceed natural recharge and produce a mining situation. This continuous overdraft may lead to undesirable effects such as increased pumping costs, land subsidence and in the case of coastal aquifers saltwater intrusion. In these situations, additional sources of surface water must be identified and brought into the area. In addition, the depleted aquifers must be recharged if groundwater is to be maintained as a viable source of water.

Spreading basins, because of their general feasibility, efficient use of space and ease of maintenance, are the most widely used technique for artificial recharge. Water is supplied to the basin and allowed to infiltrate through the bottom, slowly recharging the groundwater aquifer.

By artificially recharging an aquifer, intermediate storage is provided for withdrawals as future needs dictate. The recharged water is stored in the originally unsaturated zone between the land surface and the water table.

Previous investigations have centered around the development of an adequate description of flow below the water table. Relatively little attention has been given to an evaluation of the influence of the capillary region upon the rate of development and shape of groundwater mounds.

It is hereby intended to develop a two-dimensional model to simulate the transient response of the water table to artificial recharge

considering both capillary storage and capillary flow in the partially saturated region.

Objectives

The primary objective of this study was to evaluate the effects of capillary storage and capillary flow, in the partially saturated region, on the growth and shape of groundwater mounds from surface recharge areas. To achieve the above objective, a numerical model was developed. The numerical model incorporates an effective saturated height to simulate the effect of capillarity on storage and an effective permeable height to account for flow above the water table. The model was compared with results obtained from an existing analytical solution. In addition, the model was checked with results from a physical porous media model.

CHAPTER II

REVIEW OF LITERATURE

2.1 State of Art in Groundwater Recharge

Previously, no attempt had been made to model the effects of the capillary region above the water table in the analysis of the growth of groundwater mounds. Approximate analytical expressions, for the formation of groundwater mounds and ridges beneath spreading basins of various configurations, have been reported by many investigators. Common to most of these developments are the assumptions that the aquifer is homogeneous, isotropic and infinite in areal extent. In addition, the hydraulic properties of the aquifer remain constant with time and space, and the flow due to percolation is vertically downward until it reaches the water table.

Among the available solutions are those presented by Bauman (1952), Bittinger and Trelease (1960) and Glover (1961). In addition to the above assumptions, all the solutions are limited to a rise of the water table relative to the initial saturated depth not greater than 2 percent (Hantush, 1967).

Solutions based on a linearized differential equation in terms of the head averaged over the depth of saturation have been obtained by Hantush (1963,1967) and Marino (1974) for several different boundary conditions. These solutions are applicable where the rise of the water table relative to the initial saturated depth does not exceed 50 percent. Experimental work reported by Marmion (1962) has shown that Glover's solution is not acceptable for cases when the height of the ridge is not small relative to the initial saturated depth.

Computer models, too numerous to mention, have been developed to analyze the transient response of the water table to artificial recharge. However, no attempt was made to include the flow above the water table in any of the studies. The following sections present the significant studies on treatment of the flow in the capillary region.

2.2 Parameters Describing Capillary Properties

Many investigators have proposed empirical relationships by which capillary properties can be described, on the drainage cycle, in terms of parameters characteristic of porous media. Gardner (1958) found that the relationship between capillary conductivity and capillary pressure head for many soils seem to fit an equation of the type

$$K_e = \frac{a}{b + (P_c/\rho g)^n} \quad (2-1)$$

where K_e is the unsaturated hydraulic conductivity, $P_c/\rho g$ is the capillary pressure head, n is a constant for a given soil, and a and b are constants such that a/b is the saturated hydraulic conductivity.

Another such relationship was proposed by Arbhabhirama and Kridakorn (1968) in the form

$$K_e = K / [(P_c/P_b)^n + 1] \quad (2-2)$$

where K is the saturated hydraulic conductivity, P_b is the bubbling pressure head and n is a constant.

Equations 2-1 and 2-2 are similar except that the former is not dimensionally consistent so that the constants used depend upon the units in which the variables are expressed. Both empirical relationships were obtained on small laboratory samples. These relationships describe a smooth function that predicts a finite decrease in K_e with a finite increase in P_c within the bubbling pressure range. The reduction in

K_e just before P_b is reached is apparently a boundary effect. White et al. (1972) found that the ratio of exposed surface to volume of laboratory sample affects the capillary pressure-saturation relationship for ratios of P_c/P_b near unity. Initial desaturation of the samples occurred at exposed boundaries in a portion of the pore space which does not form a connected network of channels. Application of the data obtained from laboratory samples to field problems presents difficulties because such samples have a larger surface to volume ratio than the soil material in the field. Values of saturation and consequently K_e for a given capillary pressure would be expected to be greater in the field than for laboratory samples.

Brooks and Corey (1964) presented a method for characterizing porous media in which the dependence of permeability and saturation upon capillary pressure is expressed in terms of bubbling pressure and pore-size distribution index. According to Brooks and Corey, the relationship between effective saturation and capillary pressure for most porous materials can be expressed by:

$$S_e = (P_b/P_c)^\lambda \quad \text{for } P_c \geq P_b \quad (2-3)$$

$$\text{and } S_e = 1.0 \quad \text{for } P_c \leq P_b$$

The effective saturation, S_e , is defined by

$$S_e = (S - S_r)/(1 - S_r) \quad (2-4)$$

where S_r , the residual saturation, is the saturation at which the theory assumed the permeability is zero. The saturation, S , defined as the fraction of the pore space filled by the liquid, is related to the volumetric water content, θ , by

$$S = \theta/\phi \quad (2-5)$$

where ϕ is the total porosity.

The bubbling pressure, P_b , is defined as the minimum capillary pressure at which a continuous nonwetting phase exists. The pore-size distribution index, λ , was shown to be a measure of the relative distribution of the pore sizes and was defined as the negative slope of the straight line portion of a plot of $\log S_e$ as a function of $\log P_c/\rho g$.

The relationship between relative permeability, k_r , and capillary pressure can similarly be expressed by

$$k_r = (P_b/P_c)^\eta \quad \text{for} \quad P_c \geq P_b \quad (2-6)$$

and

$$k_r = 1.0 \quad \text{for} \quad P_c \leq P_b$$

where k_r is the ratio of the effective permeability to the saturated permeability. The relationship between λ and η has been derived theoretically and verified experimentally by Brooks and Corey and is:

$$\eta = 2 + 3\lambda \quad . \quad (2-7)$$

The mathematical expressions of equations 2-3 and 2-6 have been verified by a large number of experimental data taken from laboratory samples (Laliberte et al., 1966).

Permeability is dependent on soil properties only. Therefore, for systems where the solid matrix and fluid are assumed not to interact, the permeability, k , is related to the hydraulic conductivity by

$$K = \frac{k\rho g}{\mu} \quad (2-8)$$

where μ is the dynamic viscosity. It is apparent that the relative hydraulic conductivity, K_r , is also given by equation 2-6 since the viscosity, density and gravitational acceleration appear in both numerator and denominator.

2.3 Treatment of the Capillary Region

Although the effects of the capillary region have been formally neglected in evaluating the growth of groundwater mounds, attempts have been made by drainage engineers to somehow account for the flow within and above the capillary fringe. Donnan (1946) performed sand tank experiments to evaluate the validity of the expression

$$\frac{Q_d L}{2K} = h_c^2 - h_d^2 \quad (2-9)$$

for determining the spacing of drains. Where Q_d is the total drain outflow, L is the drain spacing, K is the saturated hydraulic conductivity of the sand, h_c and h_d are the water table elevations at the midpoint and at the drain outlet, respectively. He found that it was necessary to modify the above equation by adding the height of the capillary fringe, which was assumed to be the height above the water table at which the soil first began to desaturate, to the water table elevation in order to obtain closer agreement with experimental results. van Schilfgaarde (1970) also suggested that the water table should be increased by a constant value to account for the flow in the capillary fringe.

Chapman (1960) considered the effect of the capillary region upon discharge, height of seepage face and shape of free water surface for the case of steady flow through a bank with vertical faces. He considered the capillary flow to be confined within the capillary fringe. From comparison of his solution with the results of an electric analog, he concluded that the contribution from the capillary fringe increases as the ratio of the capillary rise to average depth of flow region is increased.

Childs (1959) and Youngs (1970) considered the case of steady drainage in equilibrium with a constant infiltration rate using a hodograph analysis. Although they considered capillary flow to be confined to the region remaining essentially saturated, the effect of the percolation rate on the height of the capillary fringe was considered. It was observed that the thickness of the capillary fringe increased with increase in infiltration rate.

Bouwer (1959) presented a concept of "critical tension" which he defined as the tension at the center of the range over which the hydraulic conductivity decreases rapidly on the equilibrium conductivity-tension curve. The elevation of the critical tension is somewhat greater than the thickness of the capillary fringe and this difference was intended to account for the flow in the partially saturated region.

When the water table rises significantly with time, as a consequence of recharge, the capillary region influences the flow a second way. The pore volume occupied by in-transit water greatly reduces the fillable pore space. The reduction in fillable voids becomes more significant as the infiltration rate is increased. In addition, as the depth to water table is decreased, the fillable voids are further reduced due to the contributions from the static moisture content profile. Both infiltration rate and depth to water table, therefore, will tend to influence the specific yield.

Glass, et al. (1977) attempted to account for the decrease in specific yield, in the zone of infiltration under a pond, in analyzing the response of the water table to artificial recharge. Based on experimental evidence of Bodman and Colman (1943) they arbitrarily assigned a specific yield to the zone of infiltration with a value equal to 20 percent

of the specific yield elsewhere in the aquifer. This artificial value of the specific yield used in their development fails to give due consideration to those parameters that can result in significant differences in the flow situation. The results of their numerical model were compared only with the linearized analytical solution of Hantush (1967). This comparison is limited to the case where the effects of the capillary region are not considered.

Luthin (1959) and Luthin and Worstell (1957) accounted for the change in specific yield with depth, in a problem of transient drainage, by taking an average of the specific yield at initial and final water table depths. The specific yield was evaluated from static water content-tension curves. It was concluded that using a constant specific yield can lead to significant errors as the water table approaches the ground surface.

Childs (1960) qualitatively described the effects of depth, precipitation rate and rate of drainage upon the specific yield. He showed that the specific yield could have values ranging from essentially zero when the water table is close to the soil surface to a constant value for very deep water tables. He also illustrated that the specific yield is significantly affected by the infiltration rate.

Duke (1972) presents a procedure for evaluating quantitatively the effect of depth to water table upon the apparent specific yield in terms of measurable soil properties. In his analysis the soil profile was in static equilibrium with the water table. His conclusions were essentially the same as those of Childs.

Schmid and Luthin (1964) applied the approach of Hooghoudt to analyze the hillside seepage problem of steady vertical recharge seeping

through the soil into a pair of parallel ditches penetrating to a sloping impermeable barrier. Although they did not explicitly evaluate the effect of capillary flow, they suggested integrating the area under the conductivity-capillary pressure curve from zero to the pressure at the soil surface, then dividing by the saturated hydraulic conductivity to obtain an equivalent depth to be added to the flow region.

Bouwer (1964) presented a method of accounting for the capillary flow suggested by Schmid and Luthin (1964). Bouwer evaluated the thickness Z_e of this fictitious capillary fringe as

$$Z_e = \frac{1}{K} \int_0^{H'} K(z) dz \quad (2-10)$$

where H' represents the depth to the water table from the soil surface, K , the saturated hydraulic conductivity, $K(z)$, the capillary conductivity and z the vertical distance measured from the water table.

Hedstrom et al. (1971) and Duke (1973) utilized this concept and a similar one related to capillary storage implied by Childs (1960) to evaluate the effect of capillary flow and capillary storage upon the performance of transient drainage systems. Since this concept will be used to analyze the growth of ground water mounds, as pertains to this investigation, the relationships developed by Hedstrom et al. and used by Duke will be discussed in the following chapter.

CHAPTER III

DEVELOPMENT OF THE PROBLEM

The growth of groundwater mounds due to vertical precolation from surface recharge areas is considered as shown in Figure 3-1. Water supplied to the basin infiltrates through the bottom under the influence of capillarity and gravity at rates less than the saturated conductivity.

When an aquifer is recharged by spreading water over an area which is underlain by a relatively impermeable stratum, a ground water mound is formed. In engineering application, the study of these profiles is of value for:

1. Predicting the amounts of lateral flow to adjacent fields or ponds.
2. Predicting the amounts of groundwater storage associated with natural or artificial recharge sites.
3. Predicting the time required for a recharged mound to decay to a given height.
4. Predicting responses of the water table at individual locations for optimizing operational recharge.
5. Predicting when the rising mound will reach the ground surface, and hence when pond intake rates will become limited by subsurface conditions.
6. Analyzing the theoretical relations in comparison with actual field observations and in determining how they are influenced by the various parameters that affect them.

Before proceeding with the formulation of the stated problem, the assumptions to be used are presented:

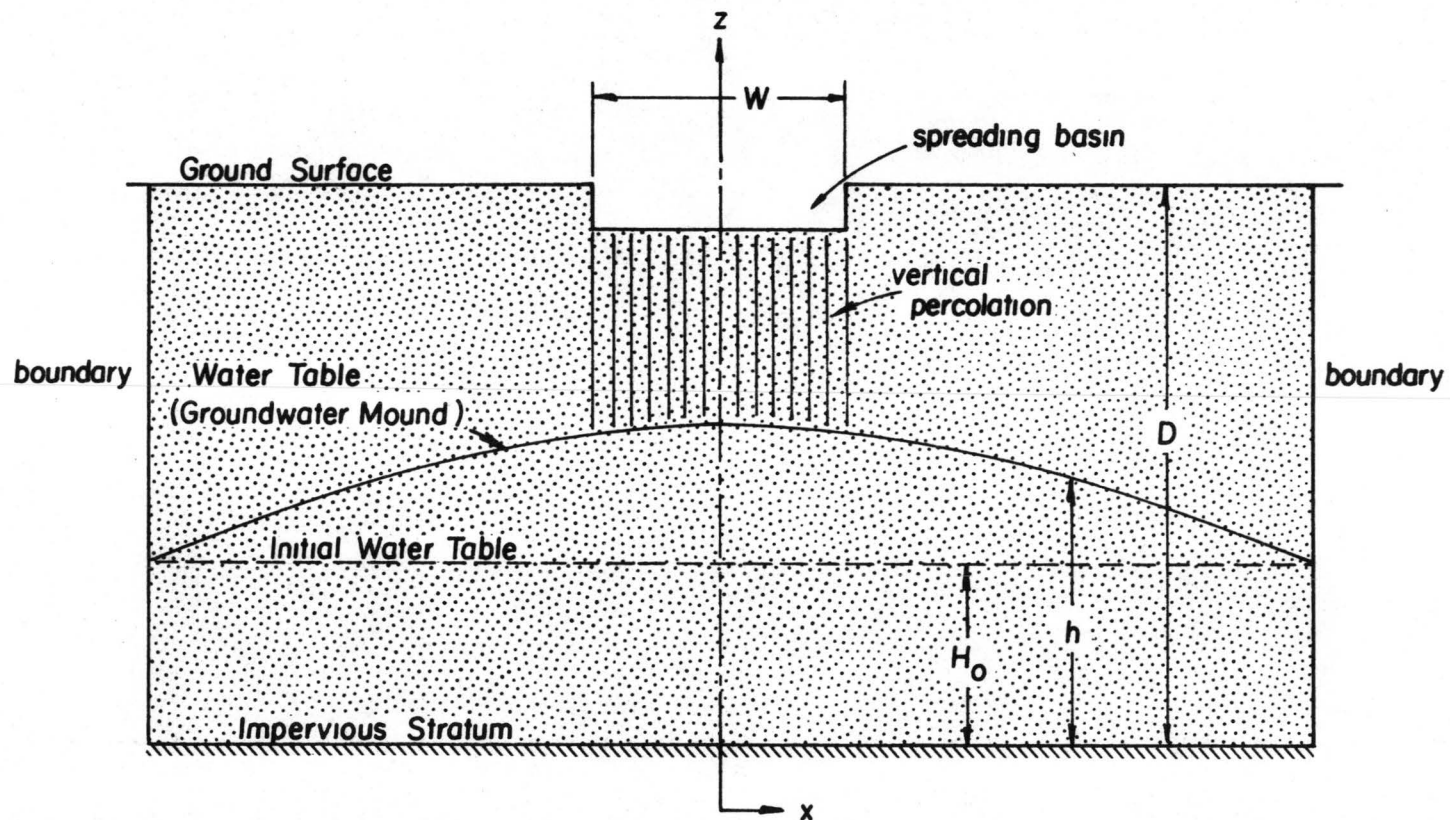


Figure 3-1. Diagrammatic representation of a groundwater mound beneath a spreading basin.

1. Constant infiltration rate so the effects of capillary hysteresis can be neglected.
2. The porous medium at any given location is homogeneous in the vertical direction, and isotropic so that the saturated hydraulic conductivity may be treated as a scalar quantity.
3. The conductivity and saturation can be described in terms of capillary pressure by the Brooks-Corey equations.
4. Soil and fluid properties remain constant with time so that the soils considered do not shrink or swell.
5. Percolation is vertically downward until it reaches the water table.
6. Vertical percolation rate is less than the saturated hydraulic conductivity and therefore the transition zone is partially saturated.

Most of this study is concerned with the use of a numerical, two-dimensional flow model, based upon the Dupuit-Forchheimer assumptions. This model has been modified to incorporate the effects of capillary storage and capillary flow for predicting mound growth in response to artificial recharge.

Based on Dupuit-Forchheimer assumptions, the differential equation describing nonsteady groundwater flow below the water table, in the presence of recharge, can be stated as follows (Eshett et al., 1965):

$$\frac{\partial}{\partial x} \left(Kh \frac{\partial H}{\partial x} \right) + \frac{\partial}{\partial y} \left(Kh \frac{\partial H}{\partial y} \right) - Q(x,y) = S_y \frac{\partial H}{\partial t} \quad (3-1)$$

where

K = saturated hydraulic conductivity

H = piezometric head

h = water table elevation referred to impermeable lower boundary

S_y = specific yield

t = time

$Q(x,y)$ = distributed source term.

To account for the changing storage capacity and conductivity in the partially saturated region, the concept of an equivalent saturated height and an equivalent permeable height is used (Hedstrom et al., 1971; Duke, 1973). In terms of the above two variables, the mass continuity equation may be modified as:

$$\frac{\partial}{\partial x} [K(h+H_k) \frac{\partial h}{\partial x}] + \frac{\partial}{\partial y} [K(h+H_k) \frac{\partial h}{\partial y}] - Q(x,y) = S_y \frac{\partial h}{\partial t} = \phi_e \frac{\partial}{\partial t} (h+H_s) \quad (3-2)$$

where

H_k = an equivalent depth of saturated soil having the same capacity for horizontal flow as the capillary region extending from the water table to the soil surface, hereon referred to as effective permeable height.

ϕ_e = drainable porosity.

H_s = an equivalent depth of saturated soil having the same volume of drainable water as the capillary region.

3.1 Equivalent Permeable Height

The effectiveness of the capillary region for transmitting horizontal flow is expressed by:

$$H_k = \frac{1}{K} \int_0^{H'} K_e dz \quad (3-3)$$

where

H' = distance from water table to soil surface,

K_e = effective conductivity.

For $H' \leq P_b/\rho g$, the effective conductivity is equal to the saturated hydraulic conductivity, hence $H_k = H'$. On the other hand if $H' > P_b/\rho g$, $K_e = K_e(z, q)$ and its magnitude will be less than the saturated conductivity above $z = P_b/\rho g$, hence $H_k \leq H'$.

The development of the equation for the effective permeable height is based upon static equilibrium considerations. The Brooks-Corey equations for effective conductivity can be expressed as:

$$K_e = K \quad \text{for} \quad P_c \leq P_b \quad (3-4)$$

and

$$K_e = K \left(\frac{P_b}{P_c} \right)^\eta \quad \text{for} \quad P_c \geq P_b \quad (3-5)$$

Under static conditions, assuming the fluid constitutes a physical continuum, the capillary pressure head is equal to the elevation above the water table. Hence, equations 3-4 and 3-5 can be written as

$$K_e = K \quad \text{for} \quad z \leq P_b/\rho g \quad (3-6)$$

and

$$K_e = K \left(\frac{P_b/\rho g}{z} \right)^\eta \quad \text{for} \quad z \geq P_b/\rho g \quad (3-7)$$

To evaluate the effective permeable height H_k , equations 3-6 and 3-7 are substituted into equation 3-3 and upon integration yields:

$$H_k = P_b/\rho g \left(\frac{\eta - H'^{1-\eta} (P_b/\rho g)^{\eta-1}}{\eta - 1} \right) \quad (3-8)$$

The depth of flow to be used in equation 3-2 would be

$$h+H_k = h + P_b/\rho g \left(\frac{\eta - H'^{1-\eta} (P_b/\rho g)^{\eta-1}}{\eta - 1} \right) \quad (3-9)$$

In order to simplify the computations of H_k , equation 3-8 may be written in terms of dimensionless variables, by dividing both H' and H_k by $P_b/\rho g$. Letting $H' = H'/(P_b/\rho g)$ and $H_k = H_k/(P_b/\rho g)$ equation 3-8 may be written as:

$$H_{k.} = \frac{\eta - H'^{1-\eta}}{\eta - 1} \quad (3-10)$$

Equation 3-10 provided a basis for evaluating the effect of capillary flow on the growth of groundwater mounds.

3.2 Equivalent Saturated Height

The influence of the partially saturated conditions upon the storage of water is analyzed by using the concept of an equivalent saturated height defined by:

$$H_s = \int_0^{H'} S_e dz \quad (3-11)$$

where S_e is the effective saturation defined by $S_e = (S - S_r)/(1 - S_r)$ and S_r is the residual saturation. The effective saturation may also be written in terms of capillary pressure as (Brooks-Corey):

$$S_e = (P_b/P_c)^\lambda \quad (3-12)$$

where λ is the pore-size distribution index. For the problem under consideration, H_s has to be evaluated from both static equilibrium and steady infiltration considerations.

For the condition when $P_c \leq P_b$ then $S_e = 1$ and $H_s = H'$. On the other hand if $P_c > P_b$ then $S_e < 1$. Therefore $H_s < H'$.

Static Equilibrium - As previously stated $z = P_c/\rho g$ for static conditions. Hence substituting equation 3-12 into equation 3-11 and noting that $S_e = 1$ for $P_c \leq P_b$ yields

$$H_s = \int_0^{P_b/\rho g} dz + \int_{P_b/\rho g}^{H'} (P_b/P_c)^\lambda d(P_c/\rho g) \quad (3-13)$$

Integrating equation 3-13 yields

$$H_s = \frac{P_b}{\rho g} + \frac{P_b}{\rho g} \left(\frac{(P_b/\rho g)^{\lambda-1} H'^{1-\lambda} - 1}{1 - \lambda} \right) \quad (3-14)$$

In terms of dimensionless variables H_s and H , equation 3-14 becomes

$$H_s = \frac{\lambda - H^{1-\lambda}}{\lambda - 1} \quad (3-15)$$

Steady Recharge - During steady recharge to the water table, the effective saturation throughout the profile below the recharge site attains a minimum value greater than the residual saturation depending upon the flux, and the capillary pressure head at every point is less than the elevation above the water table. The relationship between capillary head and elevation may be defined in terms of three separate regions bounded by z' , z'' , H' as shown in Figure 3-2 where

z' = elevation at which the capillary pressure equals the bubbling pressure,

z'' = elevation at which the effective conductivity approaches the flux in magnitude,

H' = elevation of ground surface from the water table.

Therefore, for a given profile under steady vertical flow, H_s can be expressed as follows:

$$H_s = \int_0^{z'} dz + \int_{z'}^{z''} S_e dz + \int_{z''}^{H'} S_e dz, \quad (3-16)$$

for $H' < z''$ the third integral does not exist. Before the value of H_s can be obtained, the limits of integration have to be evaluated.

By using Darcy's Law $q = -K_e \partial H / \partial z$, together with Brooks and Corey equations $S_e = (P_b / P_c)^\lambda$ and $K_r = (P_b / P_c)^\eta$ for $P_c > P_b$; also, $K_e = K$ and $S_e = 1$ for $P_c \leq P_b$; and the fact that $K_{ew} = q$ from $z = z''$ to $z = H'$; the elevations and corresponding capillary pressures at the three separate regions are evaluated as:

$$z' = \frac{1}{1+q} \quad @ \quad P_c = P_b / \rho g \quad (3-17)$$

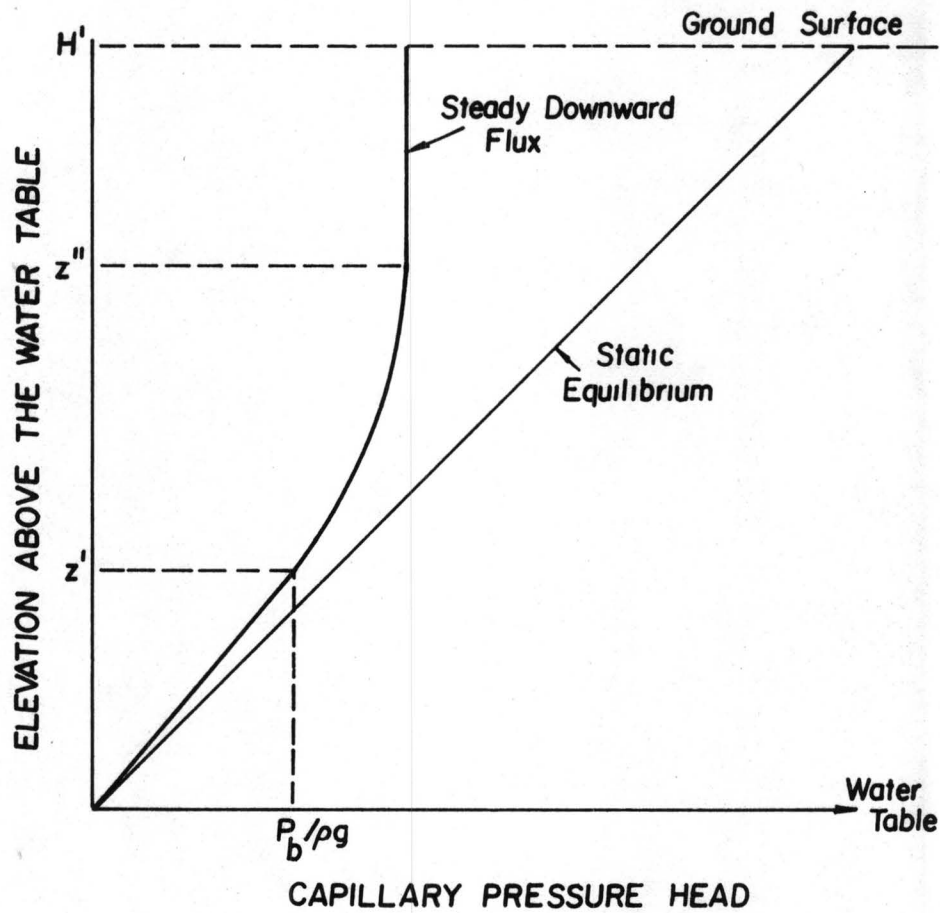


Figure 3-2. Capillary pressure profile in a soil a) in static equilibrium with a water table, b) with a steady downward flux of water.

$$z'' = \frac{1}{1+q.} + \int_1^{(-q.)^{-1/\eta}} \frac{dP.}{1+q.P.^{\eta}} \quad @ P_c = P_b/\rho g (-q.)^{-1/\eta} \quad (3-18)$$

H' = Height of ground surface above the water table

$$@ P_c = P_b/\rho g (-q.)^{-1/\eta} \quad (3-19)$$

where

$$q. = q/K$$

$$z' = z'/(P_b/\rho g)$$

$$z'' = z''/(P_b/\rho g)$$

$$\eta = 2 + 3\lambda$$

$$P. = (P_c/\rho g)/(P_b/\rho g)$$

The value of H_s can now be evaluated for the case of steady recharge by substituting the appropriate limits of integration from equations 3-17, 3-18, and 3-19 into equation 3-16 which, when integrated, yields:

$$H_{s.} = \frac{1 - (-q.)^{\lambda/\eta}}{1+q.} + (-q.)^{\lambda/\eta} H' + \int_1^{(-q.)^{-1/\eta}} \frac{P.^{-\lambda} - (-q.)^{\lambda/\eta} dP.}{1+q.P.^{\eta}} \quad (3-20)$$

Equations 3-15 and 3-20 provide a basis for evaluating the effect of capillary storage on the growth of groundwater mounds.

3.3 Development of Expression for the Specific Yield

By observing equation 3-2 in a previous section it can be seen that $S_y \partial h/\partial t$ and $\phi_e \partial(h+H_s)/\partial t$ are equal. Since the specific yield depends on the depth to the water table, by changing the order of differentiation of $\phi_e \partial(h+H_s)/\partial t$ with respect to the saturated thickness, an expression for the specific yield can be obtained in terms of ϕ_e , H_s and h , i.e.,

$$S_y \frac{\partial h}{\partial t} = \phi_e \frac{\partial}{\partial t} (h+H_s) = \phi_e \frac{\partial}{\partial h} (h+H_s) \frac{\partial h}{\partial t} = \phi_e \left(1 + \frac{\partial H_s}{\partial h}\right) \frac{\partial h}{\partial t} \quad .$$

By separating the terms we arrive at

$$S_y = \phi_e \left(1 + \frac{\partial H_s}{\partial h} \right) \quad (3-21)$$

For the case of steady recharge, the specific yield can be evaluated by substituting the appropriate expression for the equivalent saturated height (equation 3-20) into equation 3-21 which gives:

$$S_y = \phi_e \left\{ 1 + \frac{P_b}{\rho g} \frac{\partial}{\partial h} \left[\frac{1 - (-q.)^{\lambda/\eta}}{1 + q.} + (-q.)^{\lambda/\eta} H' + \int_1^{(-q.)^{-1/\eta}} \frac{P.^{-\lambda} - (-q.)^{\lambda/\eta} dP.}{1 + q.P.^{\eta}} \right] \right\} \quad (3-22)$$

If the profile is not sufficiently deep, such that $H' < z''$, then S_y is given by:

$$S_y = \phi_e \left\{ 1 + \frac{P_b}{\rho g} \frac{\partial}{\partial h} \left[\frac{1}{1+q.} + \int_1^{P_{s.}} \frac{dP.}{P.^{\lambda}(1+q.P.^{\eta})} \right] \right\} \quad (3-23)$$

where $P_{s.}$ is the dimensionless capillary pressure at the soil surface.

For the case of mound growth during recharge, the specific yield below the spreading area may be less than that adjacent to the spreading area. This is caused by the possibility of an increased moisture content of the soil below the recharge area because of in-transit water.

Hence, adjacent to the spreading area, the specific yield can be obtained by evaluating H_s , from static equilibrium consideration of the soil profile with the water table, and substituting into equation 3-21. Substituting equation 3-15 into equation 3-21 yields:

$$S_y = \phi_e \left[1 + \frac{P_b}{\rho g} \frac{\partial}{\partial h} \left(\frac{\lambda - H'!^{1-\lambda}}{\lambda-1} \right) \right] \quad (3-24)$$

Substituting the expression for H_k given by equation 3-8 into equation 3-2 yields:

$$\begin{aligned}
S_y \frac{\partial h}{\partial t} = & \frac{\partial}{\partial x} \left\{ K \left[h + P_b / \rho g \left(\frac{\eta - H' 1 - \eta (P_b / \rho g)^{\eta-1}}{\eta-1} \right) \right] \frac{\partial h}{\partial x} \right\} \\
& + \frac{\partial}{\partial y} \left\{ K \left[h + P_b / \rho g \left(\frac{\eta - H' 1 - \eta (P_b / \rho g)^{\eta-1}}{\eta-1} \right) \right] \frac{\partial h}{\partial y} \right\} - Q(x,y) \quad ,
\end{aligned}
\tag{3-25}$$

where S_y is evaluated from either equations 3-22, 3-23, or 3-24 depending on whether H_s has to be calculated based on static or steady downward flow conditions. Equation 3-25 is a differential equation for the transient response of the water table to artificial recharge accounting for the effects of capillary storage and capillary flow. The equations used in sections 3.1, 3.2 and 3.3 were presented by Duke (1973).

CHAPTER IV

NUMERICAL SOLUTION

The partial differential equation describing the transient response of the water table to artificial recharge accounting for flow and storage of water in the capillary region was solved numerically using the finite difference technique. The general computer program, for transient two-dimensional flow in a saturated water table aquifer, was developed by the professional groundwater staff at Colorado State University. The development of the model and its use have been reported by Bittinger et al. (1967), Eshett and Longenbaugh (1965), and Bibby and Sunada (1971). This program was modified to incorporate an equivalent permeable height and an equivalent saturated height to account for the effects of the capillary region on the growth of groundwater mounds. The modified numerical model RECAP1 employs a backward-difference-implicit scheme to solve the system of finite difference equations and is designed to simulate non-steady state in the two-dimensional horizontal space.

4.1 The Finite Difference Equations

The nonlinear partial differential equation describing the transient response of the water table to artificial recharge accounting for flow and storage in the capillary region may be written as:

$$\frac{\partial}{\partial x} \left(K \text{ HF } \frac{\partial H}{\partial x} \right) + \frac{\partial}{\partial y} \left(K \text{ HF } \frac{\partial H}{\partial y} \right) = SY \frac{\partial H}{\partial t} + \frac{Q}{\Delta x \Delta y} \quad (4-1)$$

where

K = saturated hydraulic conductivity (L/T),

HF = depth available for horizontal flow. This depth of horizontal flow is the sum of the water table height and the effective permeable height (L),

- H = water table elevation or piezometric head,
 referred to an established datum (L),
 SY = specific yield (dimensionless),
 Q = net groundwater withdrawal (L^3/T),
 x,y = space dimensions (L),
 t = time dimension (T).

The term HF was computed from equation 3-8, which was integrated using the Gaussian quadrature technique.

Dividing the region of groundwater flow into a rectangular grid system and using an implicit backward-difference scheme, equation 4-1, written for one grid, becomes:

$$A^t H_{i,j-1}^{t+\Delta t} + B^t H_{i,j+1}^{t+\Delta t} + C^t H_{i-1,j}^{t+\Delta t} + D^t H_{i+1,j}^{t+\Delta t} - (A+B+C+D+E)^t H_{i,j}^{t+\Delta t} = Q_{i,j}^t - E^t H_{i,j}^t \quad (4-2)$$

where

$$A^t = \frac{2K_{i,j} K_{i,j-1} \Delta Y_{i,j} \Delta Y_{i,j-1} HF_{i,j-1/2}^t}{\Delta Y_{i,j} K_{i,j} \Delta X_{i,j-1} + \Delta Y_{i,j-1} K_{i,j-1} \Delta X_{i,j}} \quad (4-3)$$

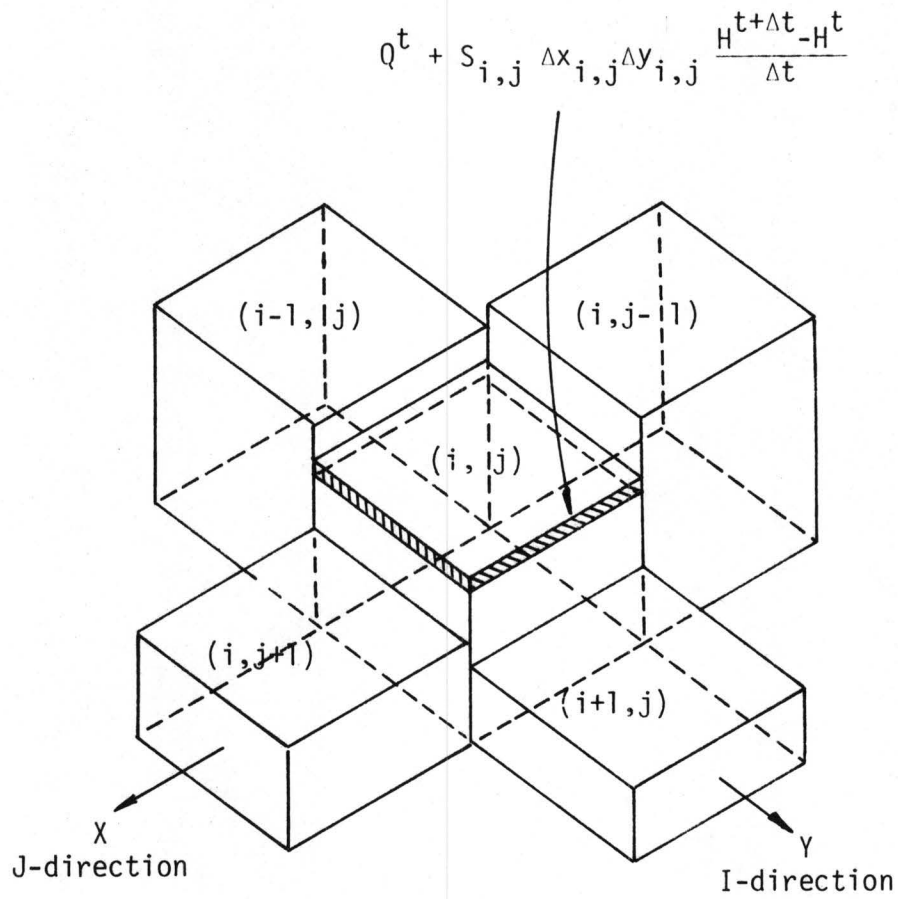
$$B^t = \frac{2K_{i,j} K_{i,j+1} \Delta Y_{i,j} \Delta Y_{i,j+1} HF_{i,j+1/2}^t}{\Delta Y_{i,j} K_{i,j} \Delta X_{i,j+1} + \Delta Y_{i,j+1} K_{i,j+1} \Delta X_{i,j}} \quad (4-4)$$

$$C^t = \frac{2K_{i,j} K_{i-1,j} \Delta X_{i,j} \Delta X_{i-1,j} HF_{i-1/2,j}^t}{\Delta X_{i,j} K_{i,j} \Delta Y_{i-1,j} + \Delta X_{i-1,j} K_{i-1,j} \Delta Y_{i,j}} \quad (4-5)$$

$$D^t = \frac{2K_{i,j} K_{i+1,j} \Delta X_{i,j} \Delta X_{i+1,j} HF_{i+1/2,j}^t}{\Delta X_{i,j} K_{i,j} \Delta Y_{i+1,j} + \Delta X_{i+1,j} K_{i+1,j} \Delta Y_{i,j}} \quad (4-6)$$

$$E^t = \frac{SY_{i,j} \Delta X_{i,j} \Delta Y_{i,j}}{\Delta t} \quad (4-7)$$

The i,j notation (see Figure 4-1) refers to the grid for which a particular equation is written and the superscripts represent the time level of computation. The term $(HF_{i,j-1/2}^t)$ in the coefficient A^t and its



$$\begin{aligned}
 & \frac{\partial}{\partial x} (K_x H F \Delta y \frac{\partial H}{\partial x}) \Delta x \\
 &= A^t (H_{i,j-1} - H_{i,j})^{t+\Delta t} \\
 &\quad - B^t (H_{i,j} - H_{i,j+1})^{t+\Delta t}
 \end{aligned}$$

$$\begin{aligned}
 & \frac{\partial}{\partial y} (K_y H F \Delta x \frac{\partial H}{\partial y}) \Delta y \\
 &= C^t (H_{i-1,j} - H_{i,j})^{t+\Delta t} \\
 &\quad - D^t (H_{i,j} - H_{i+1,j})^{t+\Delta t}
 \end{aligned}$$

Figure 4-1. Finite difference grid and its physical significance.

counterpart in the other coefficients is the depth available for horizontal flow between grid $i,j-1$ and i,j . $HF_{i,j-\frac{1}{2}}^t$ is computed by the following equation

$$HF_{i,j-\frac{1}{2}}^t = \text{MAX}(HF_{i,j}^t, HF_{i,j-1}^t) - \text{MAX}(Z_{i,j}, Z_{i,j-1}) \quad (4-8)$$

where

HF = depth available for horizontal flow referred to an established datum,

Z = bedrock elevation, referred to the same datum.

Equation 4-8 ensures that the flux out of a dry grid will be zero.

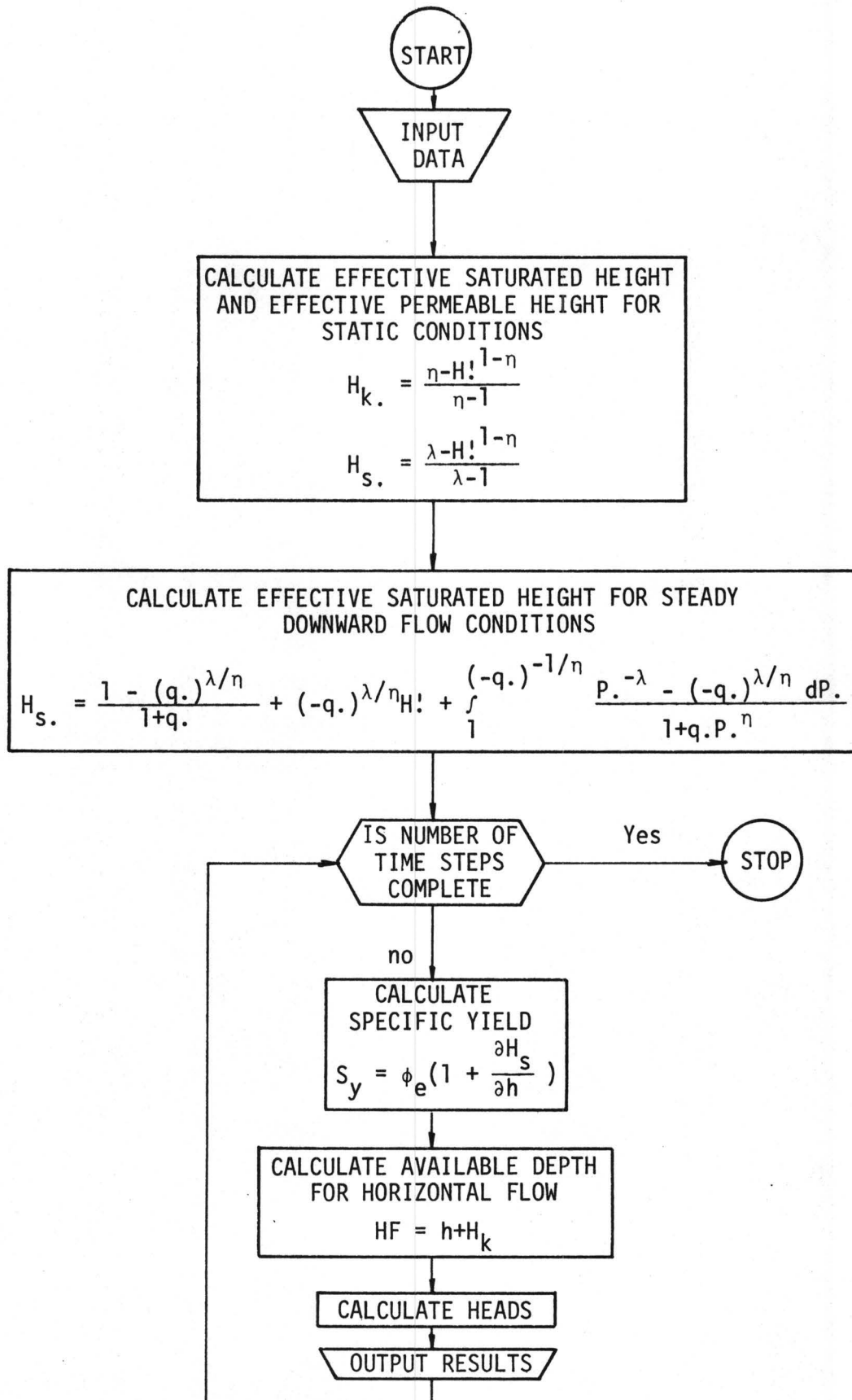
The coefficients A^t , B^t , C^t , D^t , E^t are computed at the beginning of each time increment and held constant throughout the time increment. This approximation effectively linearizes the difference equation for the unconfined case and makes solution possible. The volumetric source term, Q , where applicable, is the volume of water added through the top of each grid in a given time interval, defined as positive for flow into a grid.

4.2 Procedure For Analysis

The finite difference approach requires subdivision of the study area into a system of rectangular grids. Before initiating the computations for the first time step, the equivalent permeable height and the equivalent saturated height are evaluated for a series of water table depths and stored as arrays in the main program. These data are used to evaluate the specific yield and total flow depth for each subsequent time step until the analysis is completed. At any given time step the equivalent permeable height for each grid, corresponding to the present water table depth, is selected from this array. This height is then added to the present saturated thickness to obtain the total flow depth for the

present time step. In a similar manner the equivalent saturated height is obtained for the previous and present time steps. The specific yield is then evaluated for each grid. The implicit backward-difference form of equation 4-1 is then written for each grid as a function of the flow across each of its four faces and the net vertical withdrawal. The resulting system of equations is then solved simultaneously, using Gauss elimination, for the water table elevation at the end of the selected time step. This predicted value is then used as the initial water table elevation for the next time step and the entire process repeated. Successive solutions for the following time increments form the complete analysis. The basic sequence of events is shown in Figure 4-2. A description of the main program and each subprogram is contained in Appendix A.

Figure 4-2. Sequence of computational events.



CHAPTER V

VERIFICATION OF NUMERICAL MODEL

The numerical model used in this study is based on Dupuit-Forchheimer assumptions and utilizes the concepts of equivalent saturated and permeable heights to account for the effects of capillarity upon the growth of groundwater mounds. Before the numerical model can be used to evaluate the effects of capillary storage and capillary flow, it is necessary to demonstrate its adequacy to simulate mound growth.

To verify the adequacy of the numerical model for predicting mound heights, the results of the numerical model without capillary effects will be compared to an existing analytical solution. In addition, the numerical solution will be compared to the results of a physical model where the capillary effects are significant. The physical model will simulate the spreading of a groundwater mound due to steady recharge from a long strip of width 60 cm.

5.1 Comparison With Analytical Procedure

One method to be used in evaluating the numerical solution consists of comparing its results with those of an analytic solution, which in this case, is Glover's solution. This comparison is for the case when capillary effects are small and may be neglected.

Both solutions are based on Dupuit-Forchheimer assumptions, but Glover's solution assumes a constant flow depth throughout the recharge period thereby restricting the mound height to be very small compared to the initial saturated thickness of the aquifer. This assumption is not made in the numerical solution. To avoid any discrepancies that may arise from the preceding assumptions in Glover's solution, a large initial saturated thickness is used for this comparison.

The spreading of a groundwater mound due to a continuous recharge from a long strip of width 60 meters is considered. An impermeable boundary representing the center of symmetry and a constant head boundary are imposed at $x=0$ and $x=365$ meters, respectively. The aquifer is assumed to be bounded by a horizontal impermeable base.

Glover (1961) approached the problem by assuming that the aquifer is homogeneous, isotropic, infinite in areal extent and bounded by a horizontal impermeable base. In addition, the formation coefficients of the aquifer were assumed to be constant in both time and space, and the effects of the capillary region were neglected. The flow depth is treated as a constant throughout the recharge period thereby limiting his solution to the case where the rise of the water table relative to the initial saturated depth is small.

The equation for the one-dimensional case is

$$\alpha \frac{\partial^2 h}{\partial x^2} = \frac{\partial h}{\partial t} \quad (5-1)$$

where

h = height of the groundwater mound above the original water table level,

x = distance measured horizontally from the center of the strip,

t = time,

$\alpha = (KH_0)/\phi_e$,

and is solved for the above conditions. The resulting equation for the height of the groundwater mound at any point, x , due to continuous recharge becomes (Glover, 1961):

$$h = \frac{R}{2} \int_0^t \left(\frac{2}{\sqrt{\pi}} \int_{u_1}^{u_2} e^{-u^2} du \right) d\xi \quad (5-2)$$

where

$$u_1 = \frac{x - W/2}{\sqrt{4\alpha\xi}}$$

$$u_2 = \frac{x + W/2}{\sqrt{4\alpha\xi}}$$

$$\xi = (t-n)$$

$$R = i/\phi_e ,$$

and

n = time of application of incremental recharge,

i = uniform continuous recharge rate,

W = width of recharge strip.

The basic solution of equation 5-2 is appropriate for an aquifer of infinite areal extent. To account for the effects of the imposed boundary conditions the method of images was used.

Numerical results are compared with Glover's solution in Figure 5-1. The excellent agreement for mound heights between the two solutions is indicative of the adequacy of the numerical solution in describing the development of mound heights for the above assumptions.

5.2 Verification With Physical Model

5.2.1 Description of the physical model

The physical model is a narrow flume approximately 3.65 meters long, 40 centimeters high and 5.1 centimeters wide, containing a porous medium. The model is built of steel frames and acrylic plastic walls. A sketch of the model is shown in Figure 5-2. The upstream end has an end plate made of impermeable rubber to simulate an impermeable boundary. At the downstream end a plastic end box was attached. The retaining wall of the end box is a metal screen, which was used to provide a means by which water can leave with very small head loss.

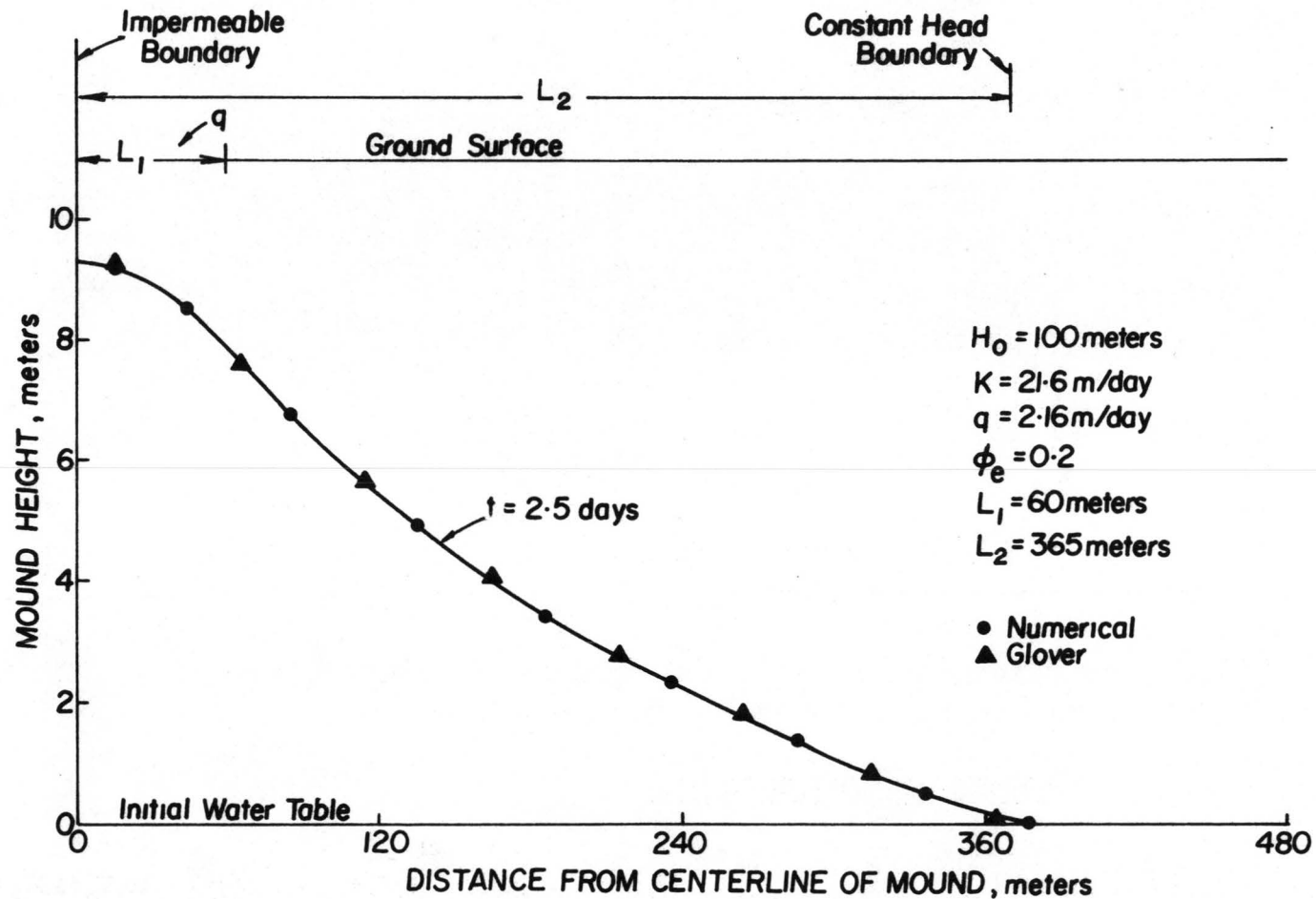


Figure 5-1. Comparison of mound shape between numerical model and Glover's solution - No capillary effects.

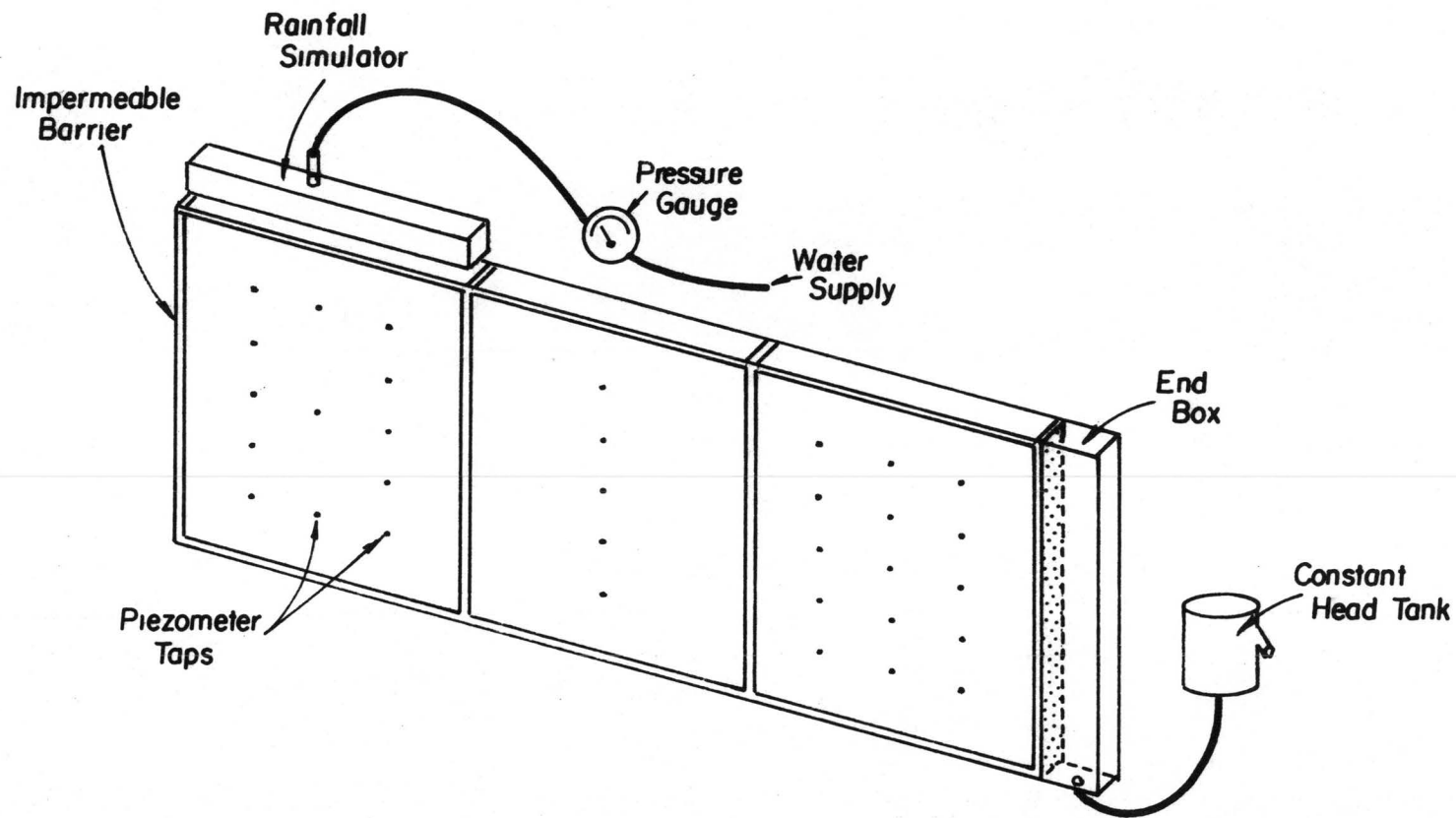


Figure 5-2. Drawing of experimental model.

The end box was provided with a drain at the bottom. The drain was connected to an adjustable constant head tank with 3/4 inch flexible tubing. This was used to simulate a constant head boundary condition. Any desired head in the end box can be maintained by sliding the adjustable constant head tank to the proper position and locking it in place with thumb screws. The overflow water from the tank is diverted to a sump through a flexible tube. A sketch of the endbox and constant head tank is shown in Figure 5-3.

5.2.2 Fluid and media

Water was used as the wetting fluid in these experiments. Two different porous media were used. One of the materials used was spherical glass beads about 2.5 mm in diameter. The glass beads are fairly uniform in size. The material is very easy to place in the model and the medium homogeneous. Data collected using the glass beads serves to check the numerical model for the effect of capillary storage. This is because the bubbling pressure head of the glass beads is very small (≈ 1 cm) and hence, the effect of horizontal capillary flow is fairly small.

The other porous material used was Ottawa sand, grade 20-30. The material was placed in the flume through a plexiglass tube 2.5 centimeters in diameter. The material was placed in layers 2-3 centimeters thick so that the packing would be as uniform as possible. Data collected using the Ottawa sand provide comparisons for the numerical model on the effects of both capillary storage and capillary flow. Since the bubbling pressure head is about 8.8 centimeters, capillary flow should be significant away from the recharge area whereas capillary storage should be significant below the recharge area.

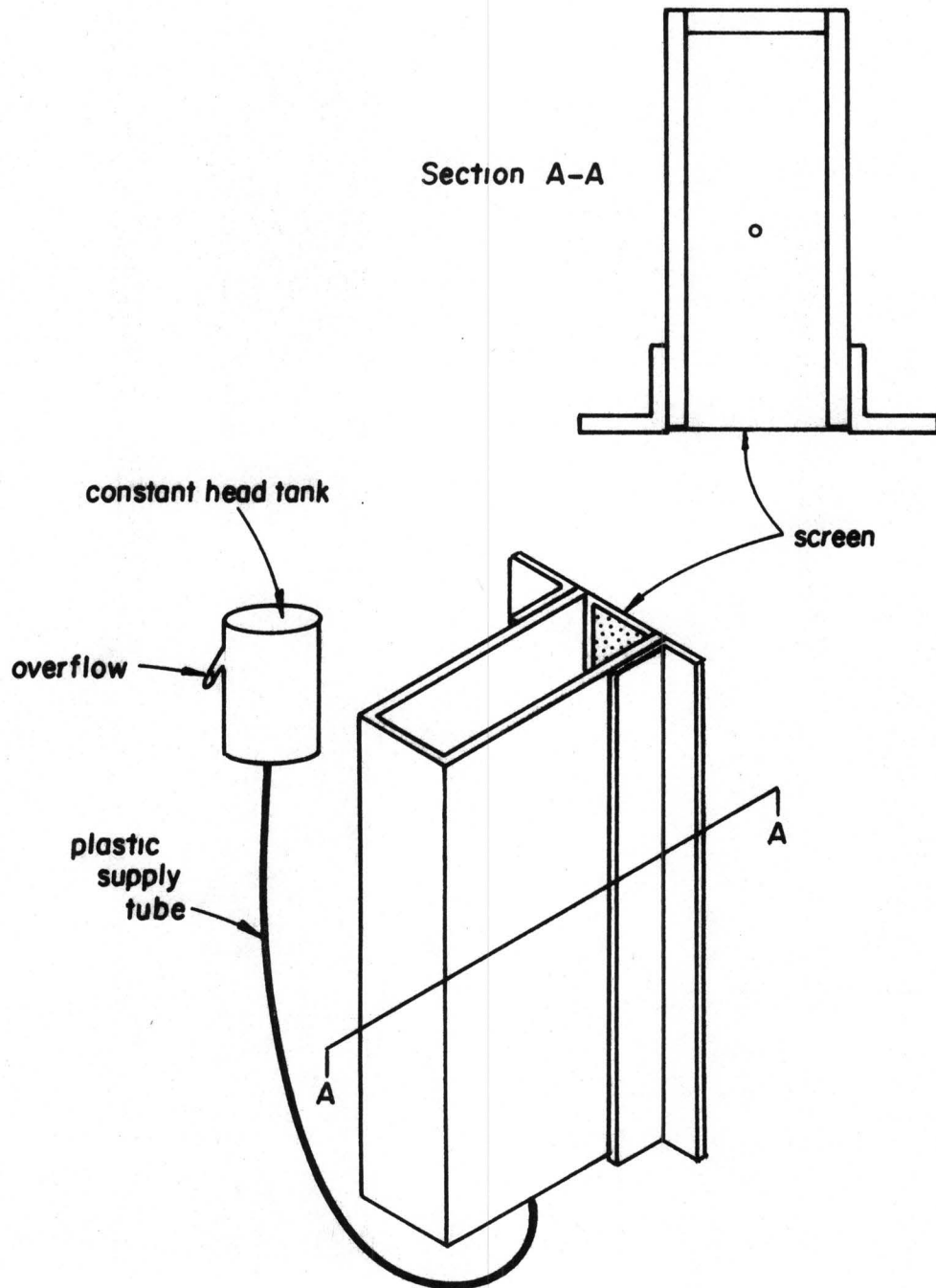


Figure 5-3. End box and constant head tank.

5.2.3 Determination of media properties

The media properties that had to be known for the experimental studies include saturated hydraulic conductivity, K , bubbling pressure, P_b , pore-size distribution index, λ , effective porosity, ϕ_e , residual water content, θ_r , and bulk density, ρ_b . All the above properties were obtained either from the capillary pressure-relative conductivity data, or from samples taken from the column used to obtain these data.

The relationship between capillary pressure head and effective conductivity was determined by using the short-column method described by Corey et al. (1965). The relative hydraulic conductivity was computed by dividing the effective conductivity by the saturated conductivity. The relationship between the relative hydraulic conductivity and capillary pressure head for the Ottawa sand is shown in Figure 5-4.

The bubbling pressure head and the pore-size distribution index were determined from Figure 5-4, following the procedure described by Laliberte et al. (1966). The bubbling pressure head is obtained by extrapolating a straight line to the ordinate axis where the relative hydraulic conductivity equals unity. From the negative slope of the straight line portion of the curve, the parameter η is obtained. The pore-size distribution, λ , is then calculated from the relationship $\eta = 2 + 3\lambda$.

The total porosity of the material in the flume was determined by utilizing the bulk density, ρ_b , of the medium and the particle density, ρ_s , and the relationship,

$$\phi = 1 - \rho_b / \rho_s \quad . \quad (5-3)$$

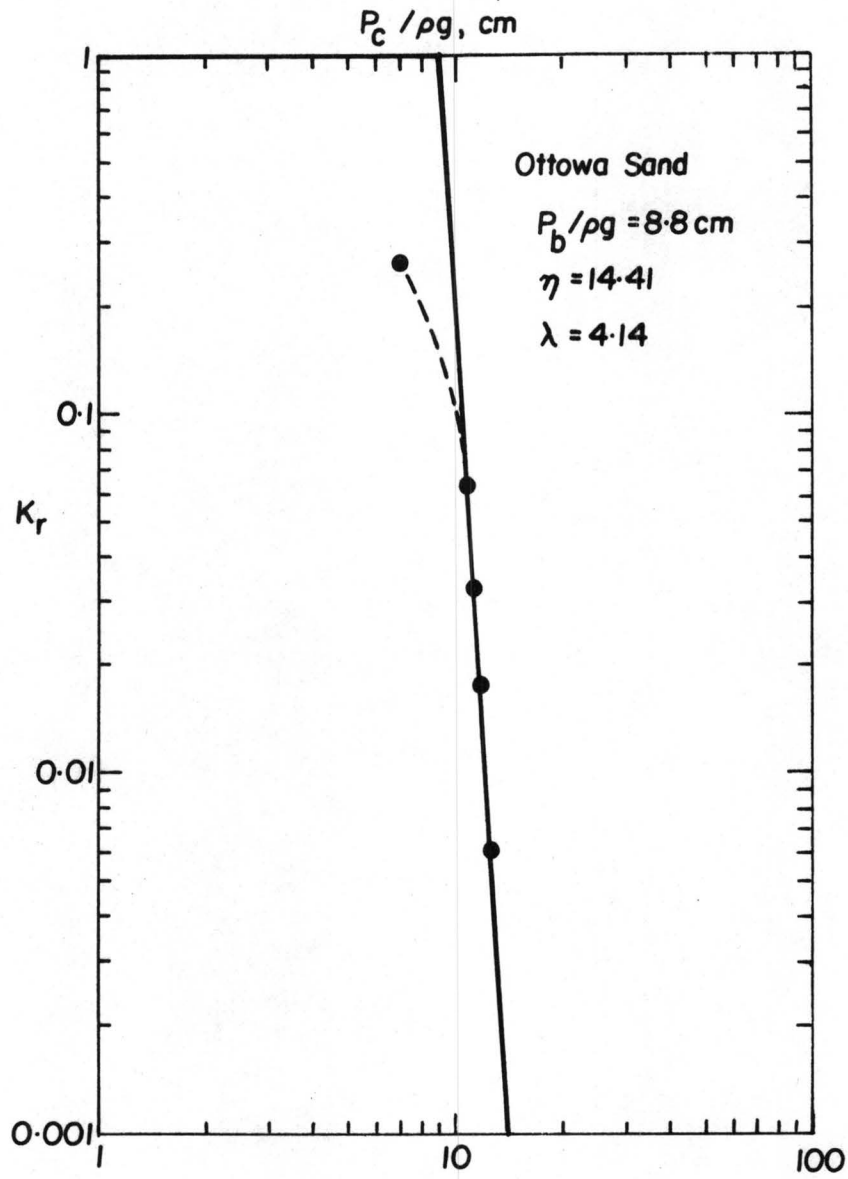


Figure 5-4. Relative conductivity as a function of capillary pressure head.

The bulk density was measured by dividing the gross weight of air-dry sand in the flume by the known volume occupied by the material. The particle density was measured by the pycnometer method.

The residual moisture content was determined from the test section by allowing the column to drain for three days to a suction of approximately one meter after the completion of an experiment. Knowing the dry weight, volume and weight of sample after three days gravity drainage, the residual water content was computed. The effective porosity ϕ_e was determined from the relationship

$$\phi_e = \phi - \theta_r \quad . \quad (5-4)$$

The hydraulic properties of the porous media used in these experiments are presented in Table 5-1.

Table 5-1. Properties of Porous Material

Type	K_{sat} cm/sec	$P_b/\rho g$ cm	ϕ_e	λ	Grain size mm	Description
Glass beads	5.066	1.0	0.32	7.0	2.5	Industrial Glass beads Type V-110
Sand	0.65	8.8	0.20	4.14	pass 20 ret. 30 ASTM	Ottawa sand

5.2.4 Measurement of hydraulic head in the model

The hydraulic head in the model was measured to locate the position of the water table. Piezometers, installed in one sidewall of the model, were used to measure the hydraulic head. The number of piezometers used at any given time depended on the position of the water table. For any given run the maximum number of piezometers used was 20. The piezometer system consisted of seven columns, six columns with five piezometers 6.4 centimeters apart, and one column with three piezometers (see Figure 5-2).

Each piezometer is constructed from a 5/8 inch diameter bolt bored along its axis. Disc-shaped nylon screen is sealed to the threaded end of each bolt. The piezometers are screwed into the sidewall of the model with very small penetration into the medium. A seal between the bolts and the model wall was obtained with O-ring seals. A view of the piezometer is shown in Figure 5-5.

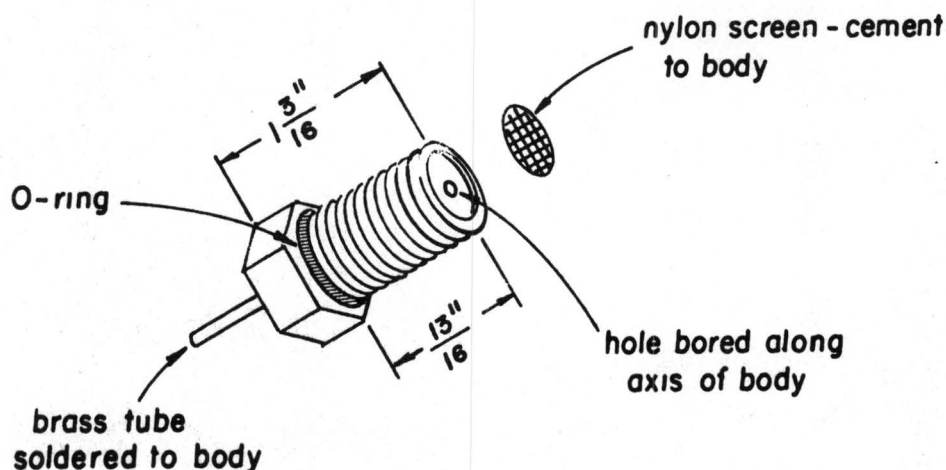


Figure 5-5. View of Piezometer.

The manometers are capillary glass tubes mounted on a board. Flexible plastic tubing was used to connect the brass tubing in the piezometer to the manometers. To obtain the hydraulic head it was found necessary to photograph the manometer board instead of taking the measurements directly from the manometers to obtain simultaneous measurements of all piezometers.

5.2.5 Recharge experiment

The initial condition for each recharge test was that of a horizontal water table at a previously selected elevation. This was achieved

by observing the piezometric head levels from a row of seven piezometers to insure that no detectable initial hydraulic gradients existed.

When the correct hydraulic head had been established, a constant recharge rate was started at the soil surface using a rainfall simulator. The simulator, 60 centimeters long, 6 centimeters wide and 4 centimeters high, was located at the upstream end of the model. The recharge rate was set by adjusting the pressure gauge, mounted at the top of the flume, to a given pressure. The pressure readings were then converted to volumetric units from the calibration curve obtained for the simulator. During a test, the pressure gauge was continuously observed and the flow corrected to minimize variations in discharge throughout the test. The hydraulic head was obtained by photographing the manometer board at suitable intervals of time. These readings were continued until the water table beneath the recharge area was approximately one bubbling pressure head below the soil surface.

5.2.6 Comparison with physical model

Data from the physical model on the growth of the mound for the two series of tests are given in Appendix B and a portion of the data, typical of the results obtained, is plotted in Figures 5-6, to 5-9. Figures 5-6 and 5-7 present data for the glass beads at two different times. Since the bubbling pressure head for the beads is only one centimeter and the pore-size distribution index is 7.0, the effective permeable height will, according to equation 3-10, be small compared to the initial saturated thickness of 14.35 centimeters. Consequently, the effect of capillary flow will be small since it is directly proportional to the magnitude of the effective permeable height. The results from the glass beads will serve to evaluate the numerical model in its ability to

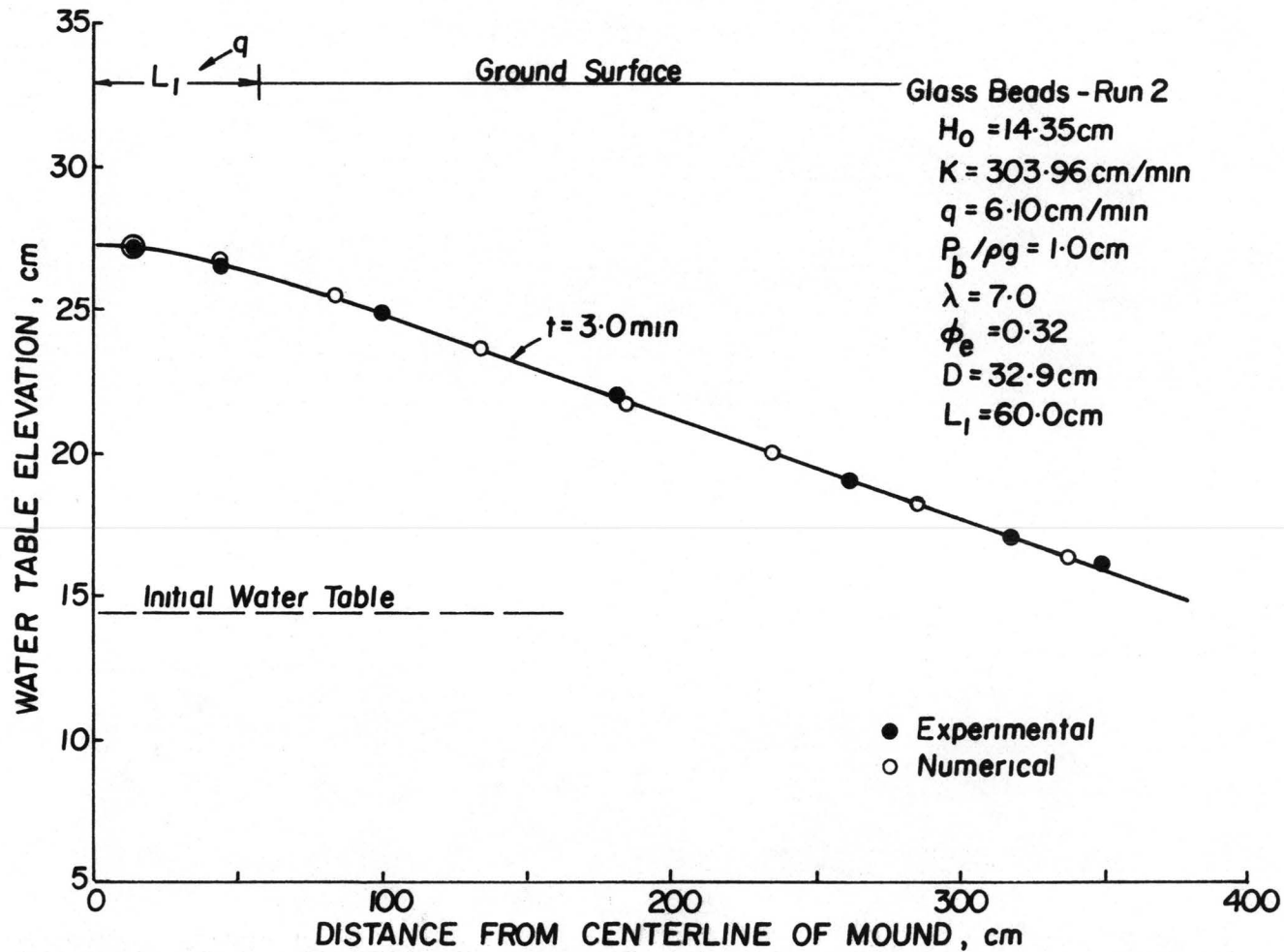


Figure 5-6. Comparison of mound shape between numerical model and experimental results.

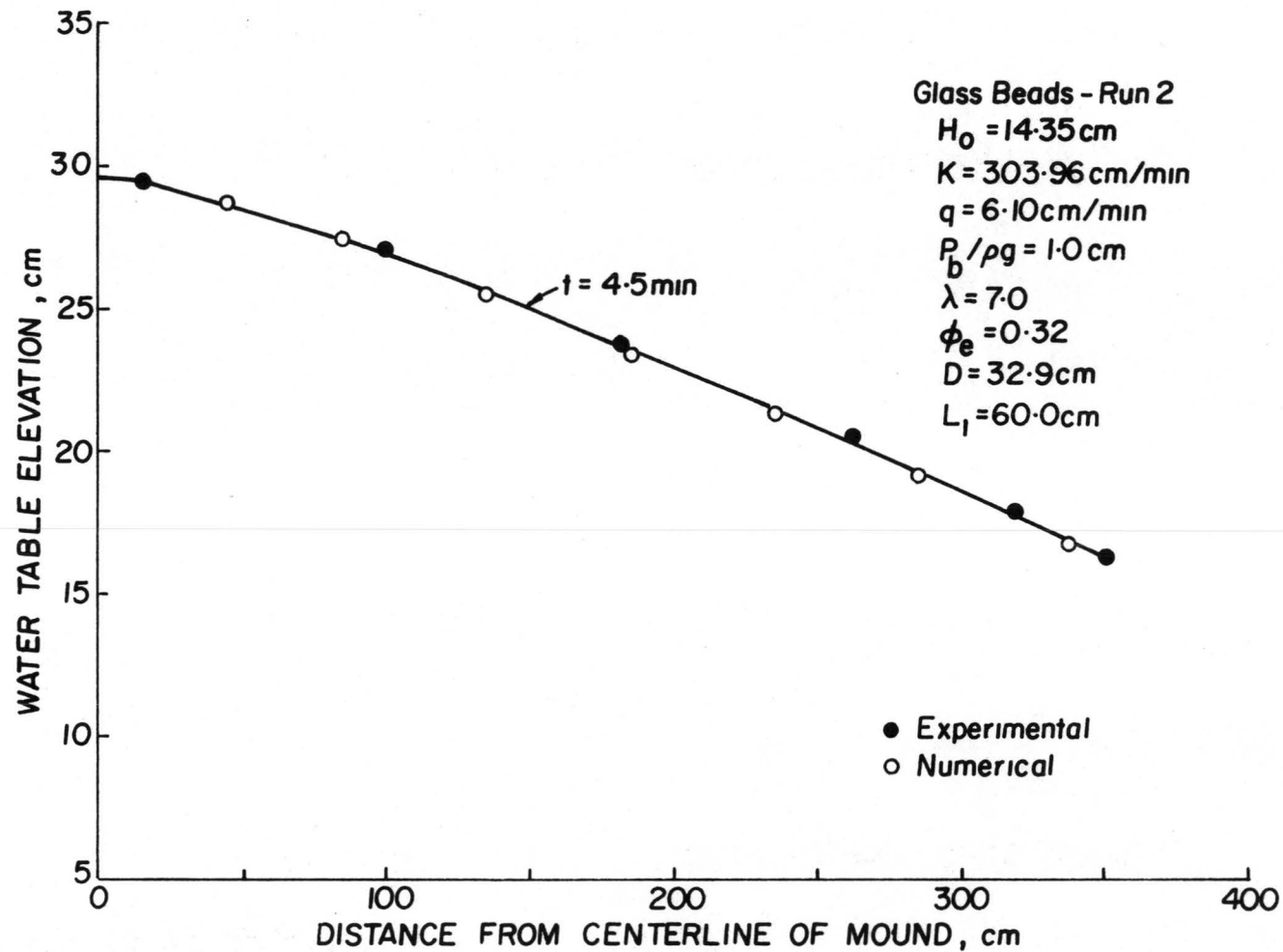


Figure 5-7. Comparison of mound shape between numerical model and experimental results.

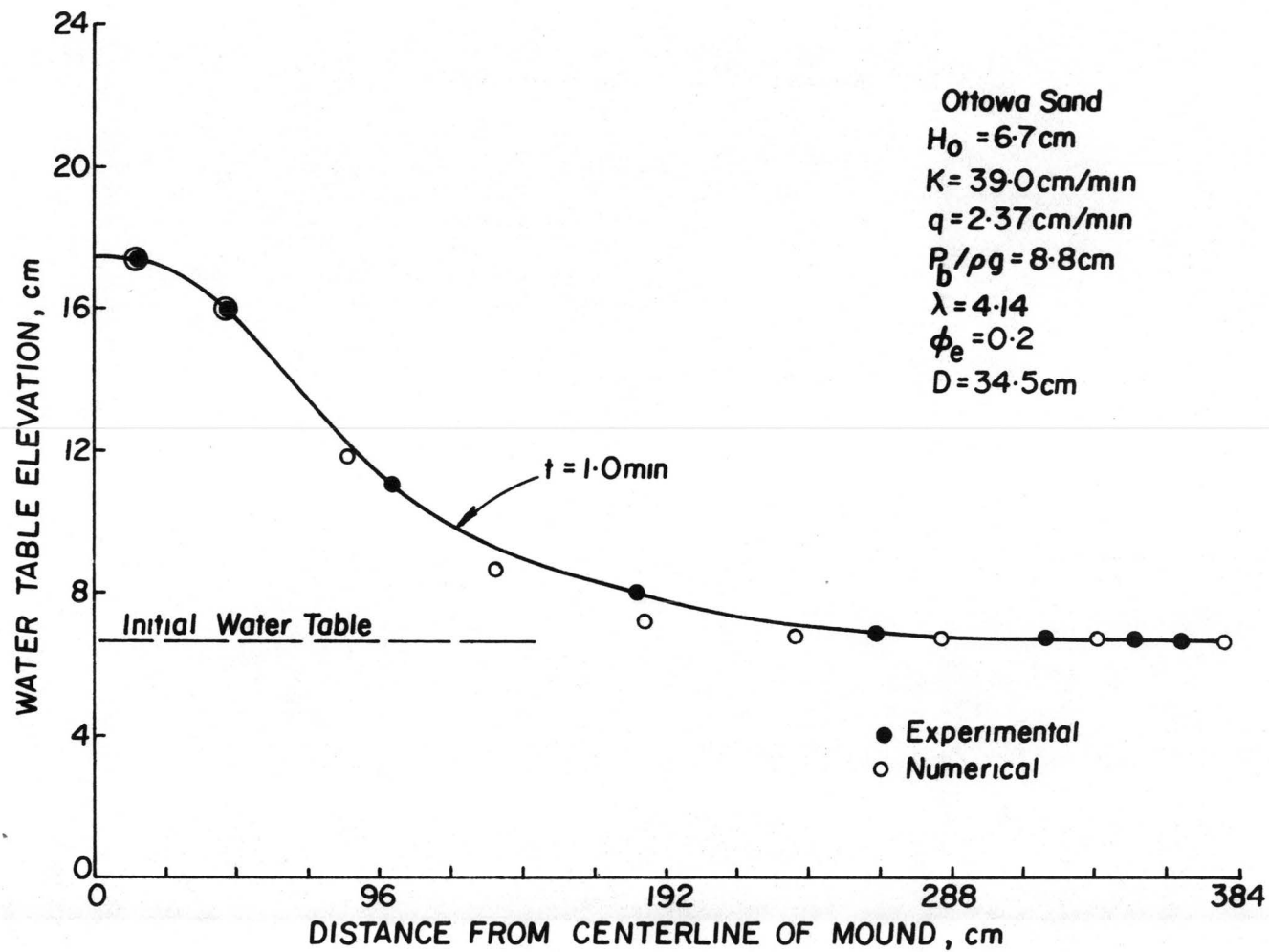


Figure 5-8. Comparison of mound shape between numerical model and experimental results.

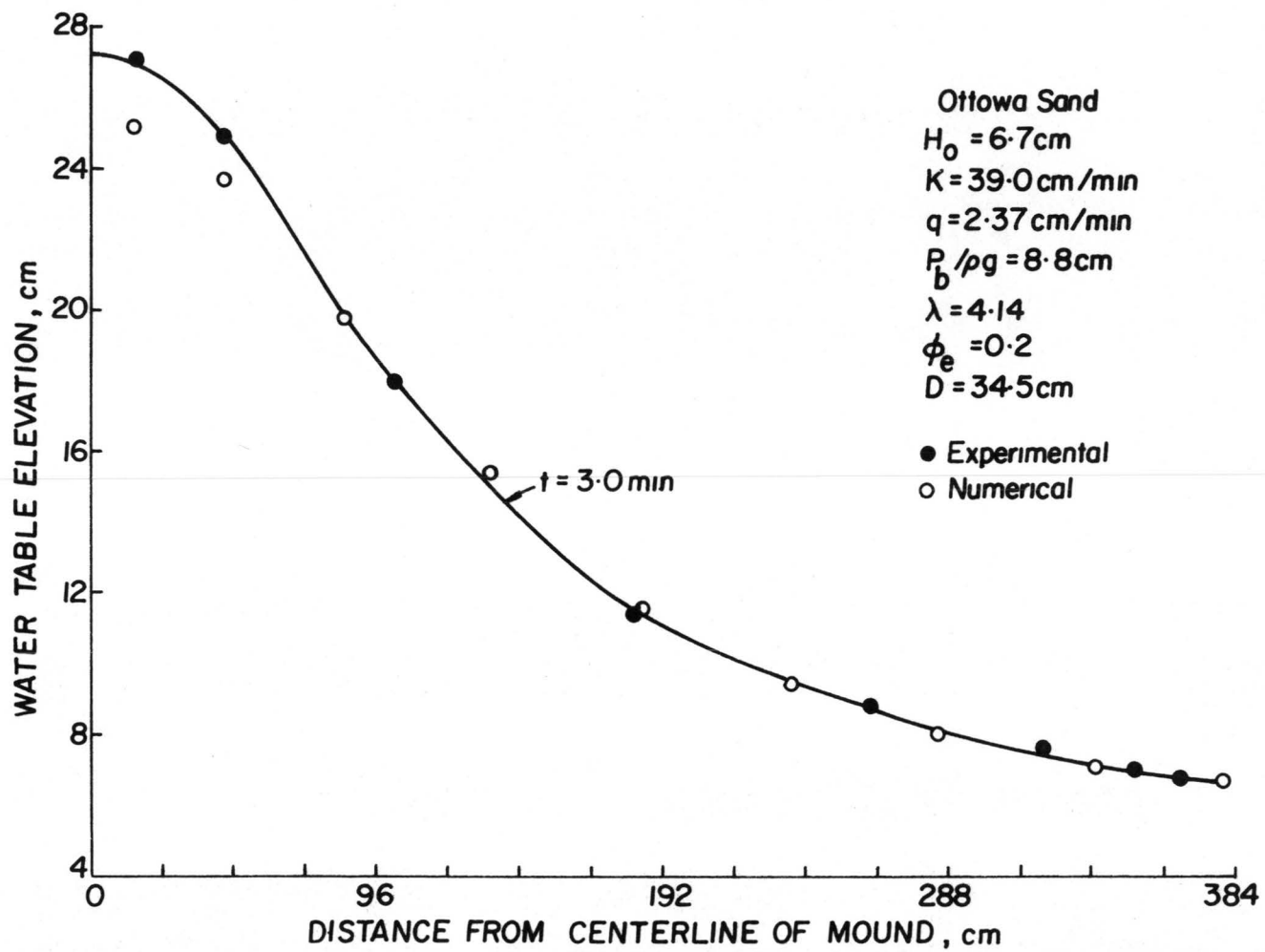


Figure 5-9. Comparison of mound shape between numerical model and experimental results.

simulate the effects of capillary storage. It is apparent from Figures 5-6 and 5-7 that the agreement that exists between both models at early and later times is quite good.

Figure 5-8 and 5-9 present data for the Ottawa sand. Since the bubbling pressure head for the sand is 8.8 centimeters, which is the same order of magnitude as the initial saturated depth of 6.7 centimeters, the effect of capillary flow is significant. The results from the Ottawa sand will, therefore, serve to evaluate the ability of the numerical model in simulating mound growth when both capillary storage and capillary flow are significant. Figure 5-8 shows that for the Ottawa sand comparable agreement exists between the numerical solution and experimental results at early times. However, at later times a lesser degree of coalescence exists below the recharge area and some scatter is observed in the proximity of the toe of the mound as shown in Figure 5-9.

Local nonhomogeneity, as discussed by Smith (1970), may contribute to the scatter of experimental data. The lower mound heights predicted by the numerical model below the recharge area may be attributed to the fact that the numerical model does not consider the effects of vertical gradients. Also, the reduction in porosity due to entrapped air as discussed by Hanson (1977) is not considered. Thus, one would expect the actual mound heights to rise more rapidly than predicted.

It should be noted that the results from the numerical model were obtained from actual soil properties determined in a separate laboratory test and not by calibrating the numerical model. The above comparisons between experimental and numerical results are considered sufficiently

accurate to justify further use of the numerical model in evaluating the effects of capillarity on the growth of groundwater mounds.

CHAPTER VI

RESULTS AND DISCUSSION

The primary objective of this study is to illustrate how capillary storage and capillary flow in the partially saturated region affect the growth of groundwater mounds under steady recharge. To achieve this objective the numerical model, which has been verified with a physical model, will be used to generate a series of solutions to illustrate the effects of capillarity. Although the numerical model is capable of simulating mound growth in the two-dimensional horizontal space the solutions to be presented are for the one-dimensional case of strip recharge as this is the condition under which the numerical model was verified.

6.1 Influence of the Capillary Region on Analytical Solutions

Present analytical solutions are based on the assumptions that the water table effectively bounds the permeable region and that the fillable pore space is independent of soil water pressure and, therefore, is a constant typically equal to the drainable porosity. This amounts to neglecting the effects of the capillary region. To illustrate the significance of these assumptions on the growth of groundwater mounds due to steady recharge, Glover's solution will be compared with the results of the numerical solution and the experimental test. This comparison is presented in Figure 6-1 using the experimental model dimensions.

From Figure 6-1, it is apparent that Glover's solution does not compare with either the experimental or numerical model results. The large discrepancies in Glover's solution are due primarily to the development of large mound heights as compared to the initial saturated thickness. Also, the constant saturated depth assumed in Glover's solution will reduce the flow away from the recharge area thereby forcing Glover's

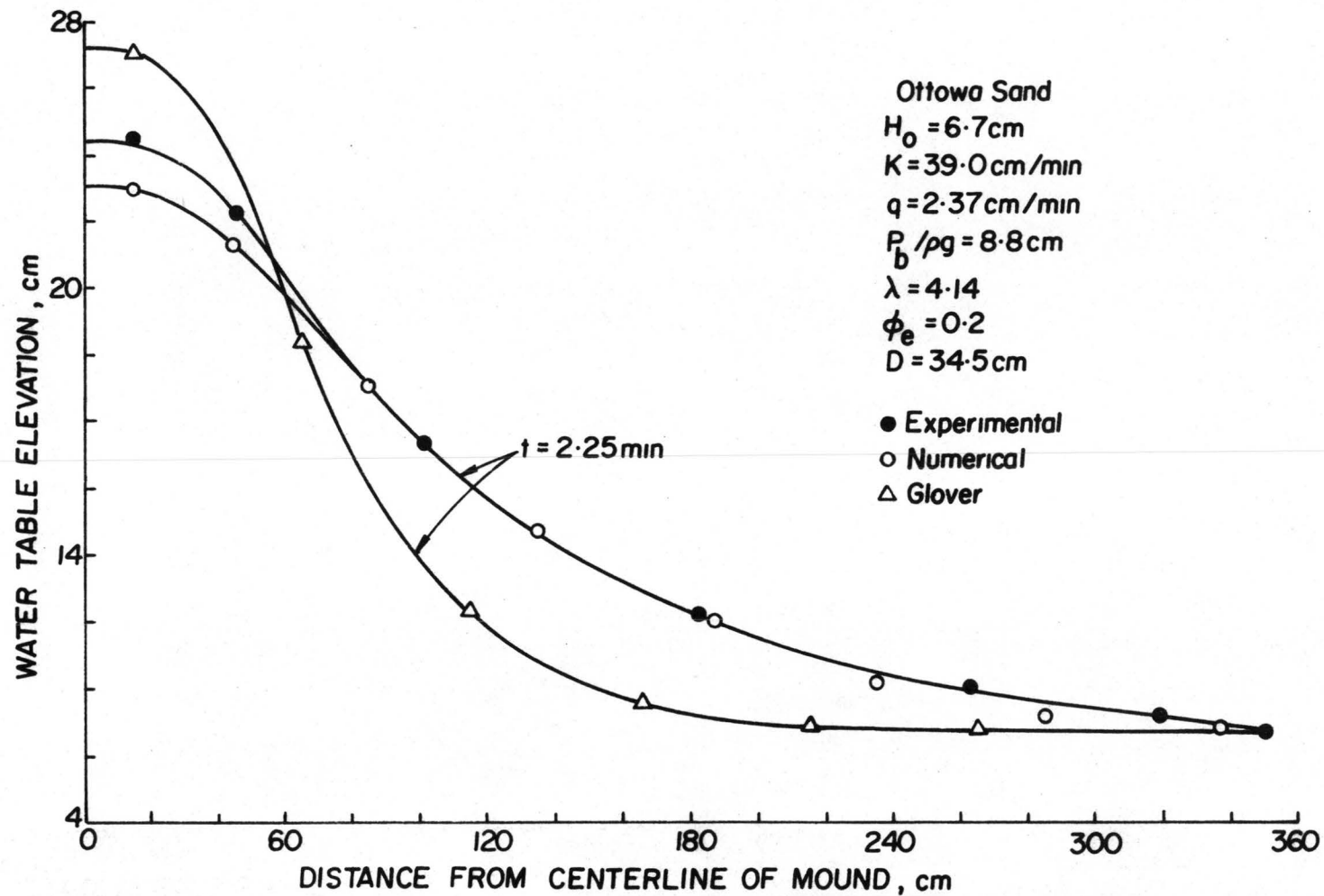


Figure 6-1. Comparison of mound shape between experimental and numerical model and Glover's solution.

solution to be higher than either numerical model or experimental results beneath the recharge site and lower away from the recharge area.

It is interesting to evaluate the effects of the capillary region when the mound heights are small compared to the initial saturated thickness. To illustrate this condition the numerical model results are compared to Glover's solution in Figures 6-2 and 6-3 for prototype dimensions of $L_1 = 100$ meters, $K = 86.4$ meters/day, $\phi_e = 0.2$, $q = 2.59$ meters/day and $H_0 = 80$ meters. It is apparent from Figure 6-2 that Glover's equation underestimates the central mound height by as much as 48 percent at early times and 16 percent at later times. The reason for this discrepancy is due primarily to a reduction in specific yield not accounted for in Glover's solution. It can also be noted that the magnitude of the error increases with time.

The depth available for horizontal flow, as predicted by the numerical model, is larger than Glover's constant saturated depth. Consequently, Glover's solution underestimates the flow away from the recharge site. As a result of the decrease in volume of water to be stored, the mound height obtained from Glover's equation is smaller away from the recharge area. The magnitude of the error increases with time as the water table approaches the ground surface. However, the relative error decreases from 56 percent at early times to 24 percent at later times. This evaluation is shown in Figure 6-3 at 150 meters from the edge of the recharge site. The above analyses indicate that neglecting the effects of capillarity can lead to significant errors in the prediction of mound height both beneath and away from the recharge site.

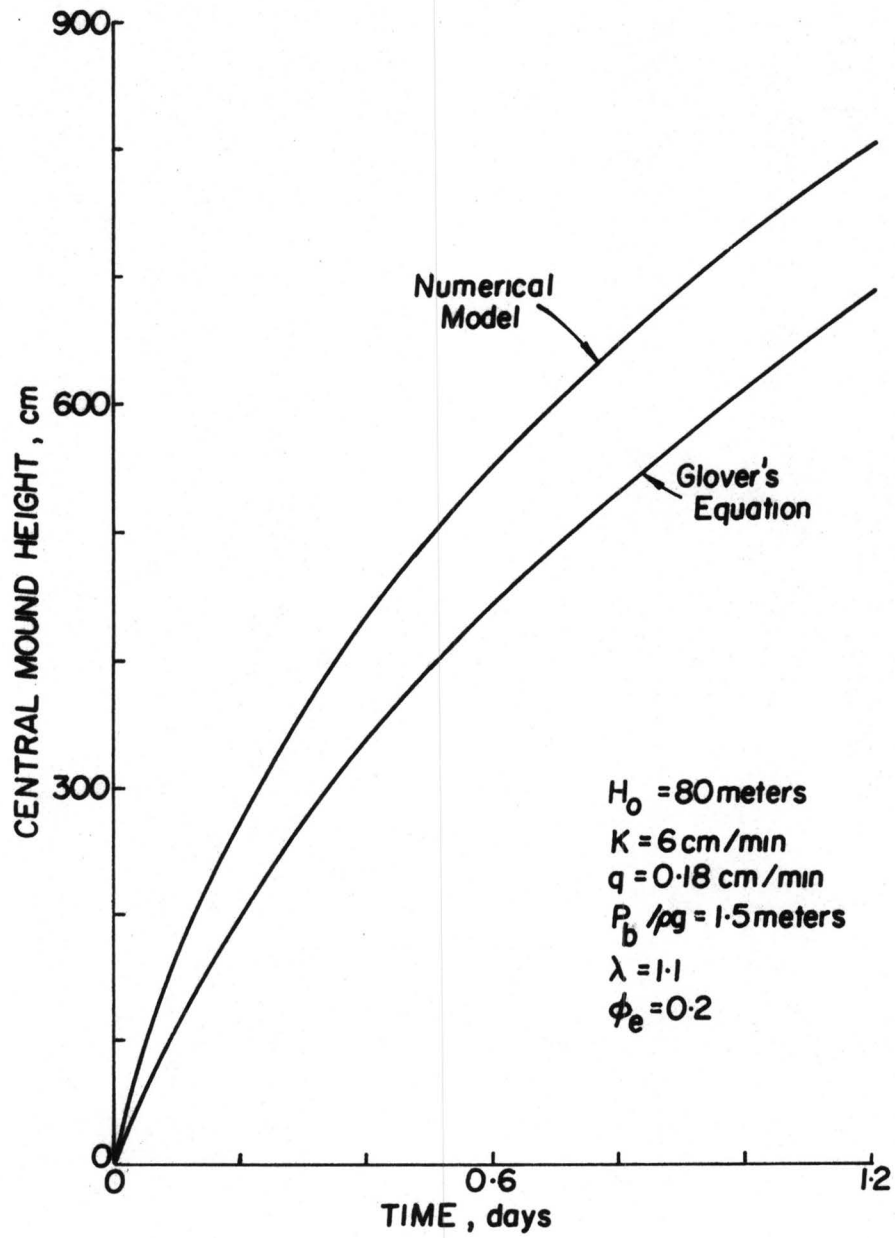


Figure 6-2. Comparison of central mound height between numerical model and Glover's equation.

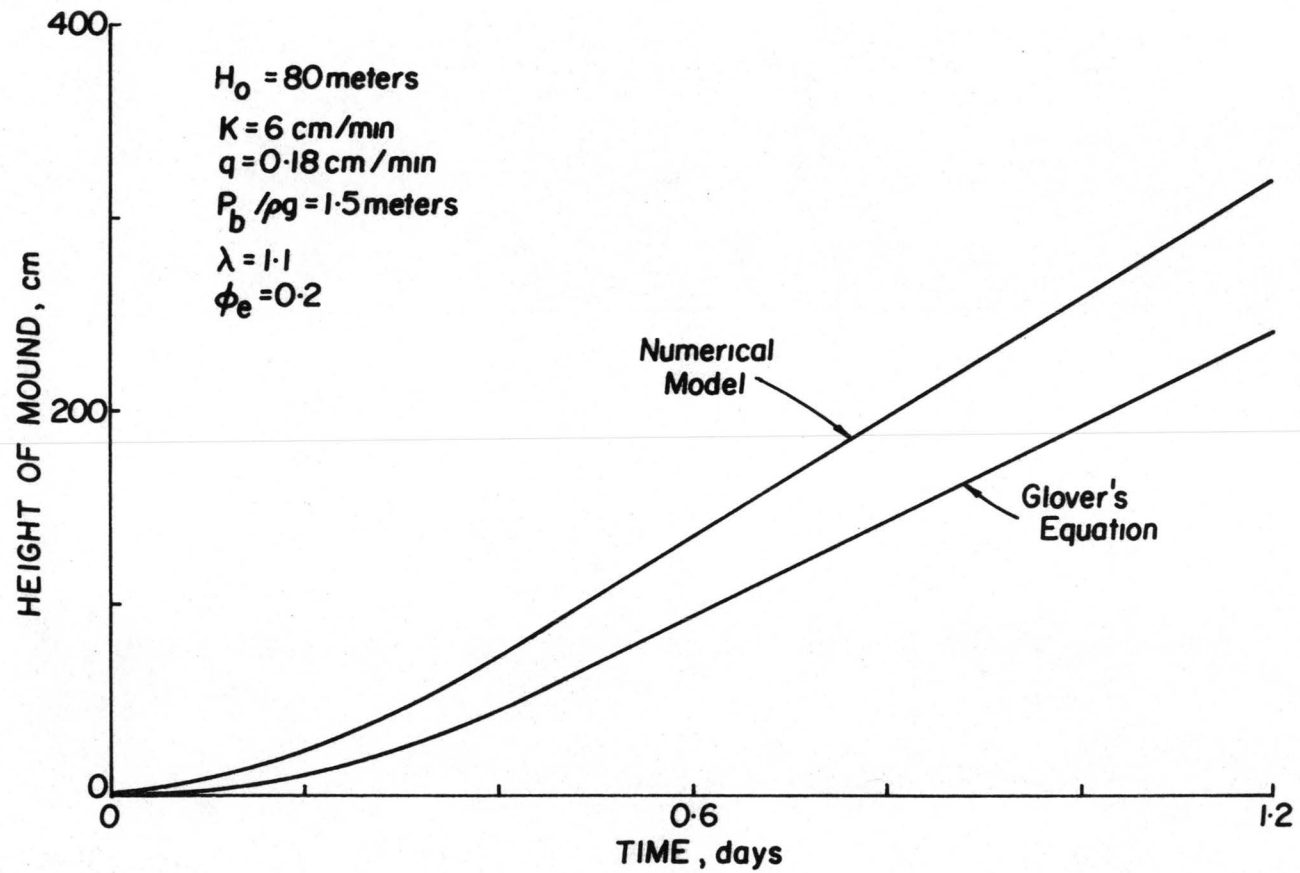


Figure 6-3. Comparison of mound height between numerical model and Glover's solution at 150 meters from edge of recharge area.

6.2 Mound Growth Evaluation

The numerical model was used to generate a series of solutions for different boundary and initial conditions, soil properties and recharge rates to evaluate the growth of groundwater mounds. The remainder of this study is concerned with the analysis of the generated data.

6.2.1 Influence of capillary storage and capillary flow

The contribution of the capillary region on the transient response of the water table to artificial recharge depends on both capillary storage and capillary flow. Under steady downward flow conditions the pore volume occupied by in-transit water greatly reduces the fillable pore space. For deep water tables the reduction in fillable voids is dependent on the infiltration rate only. On the other hand, as the water table approaches the ground surface, the contribution from the static moisture content profile further decreases the fillable pores. Consequently, capillary storage is dependent on in-transit water and the contribution from the static moisture content profile. The numerical model RECAP1, developed for this study, can simulate no capillary effects ($H_k=0$, $H_s=0$), no capillary flow ($H_k=0$), no capillary storage ($H_s=0$), the influence of in-transit water only ($P_b/\rho g = 0$), or the combined effect of capillary storage and capillary flow.

Figure 6-4 illustrates the relative importance of the capillary region on central mound height. For the conditions shown it is apparent that capillary storage is more important than capillary flow. Since in practical situations the piezometers are installed away from the recharge plot, it is interesting to evaluate the effects of the capillary region beyond the recharge boundaries. Figure 6-5 shows one such evaluation at 150 meters from the edge of the recharge area. It is evident that the

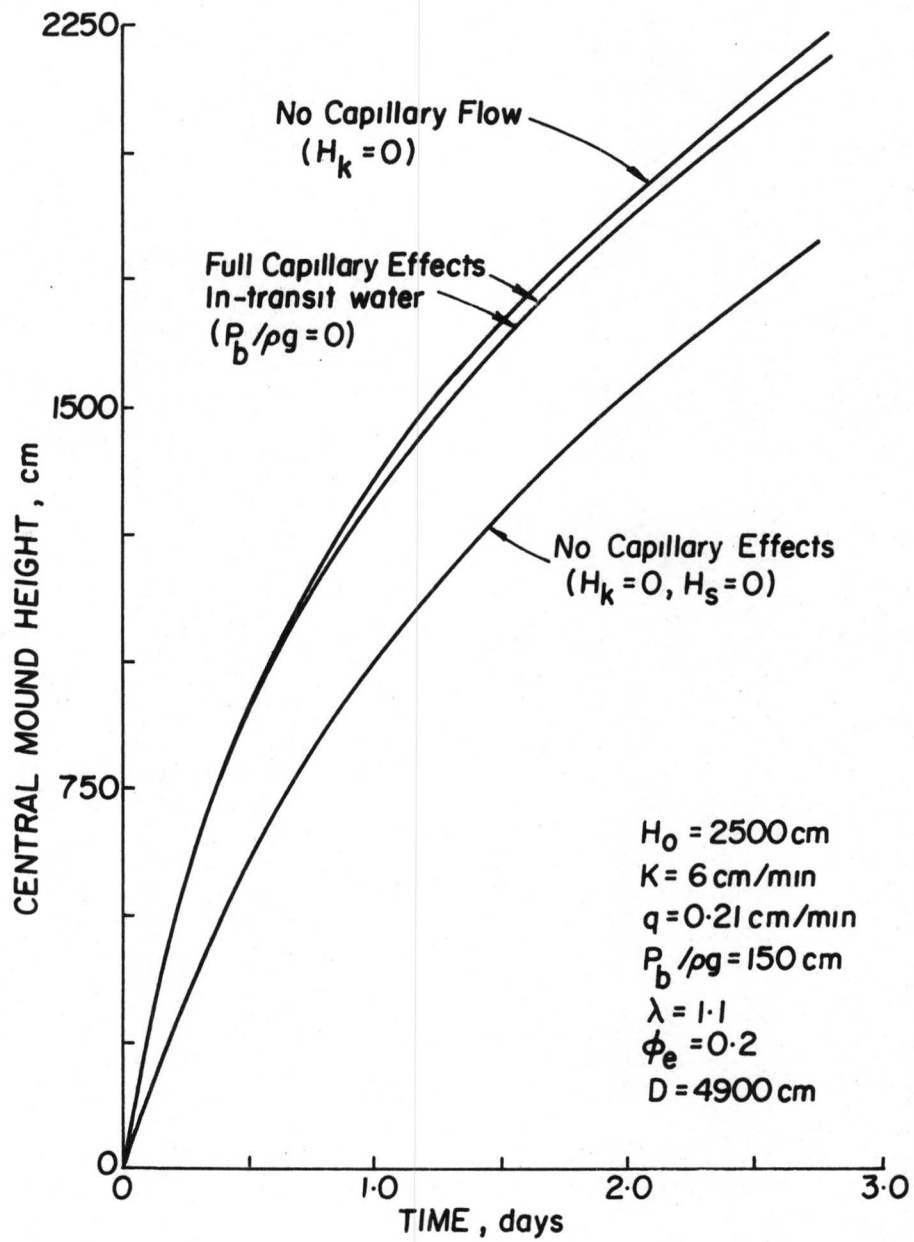


Figure 6-4. Comparison of the relative importance of capillary flow and capillary storage on central mound height.

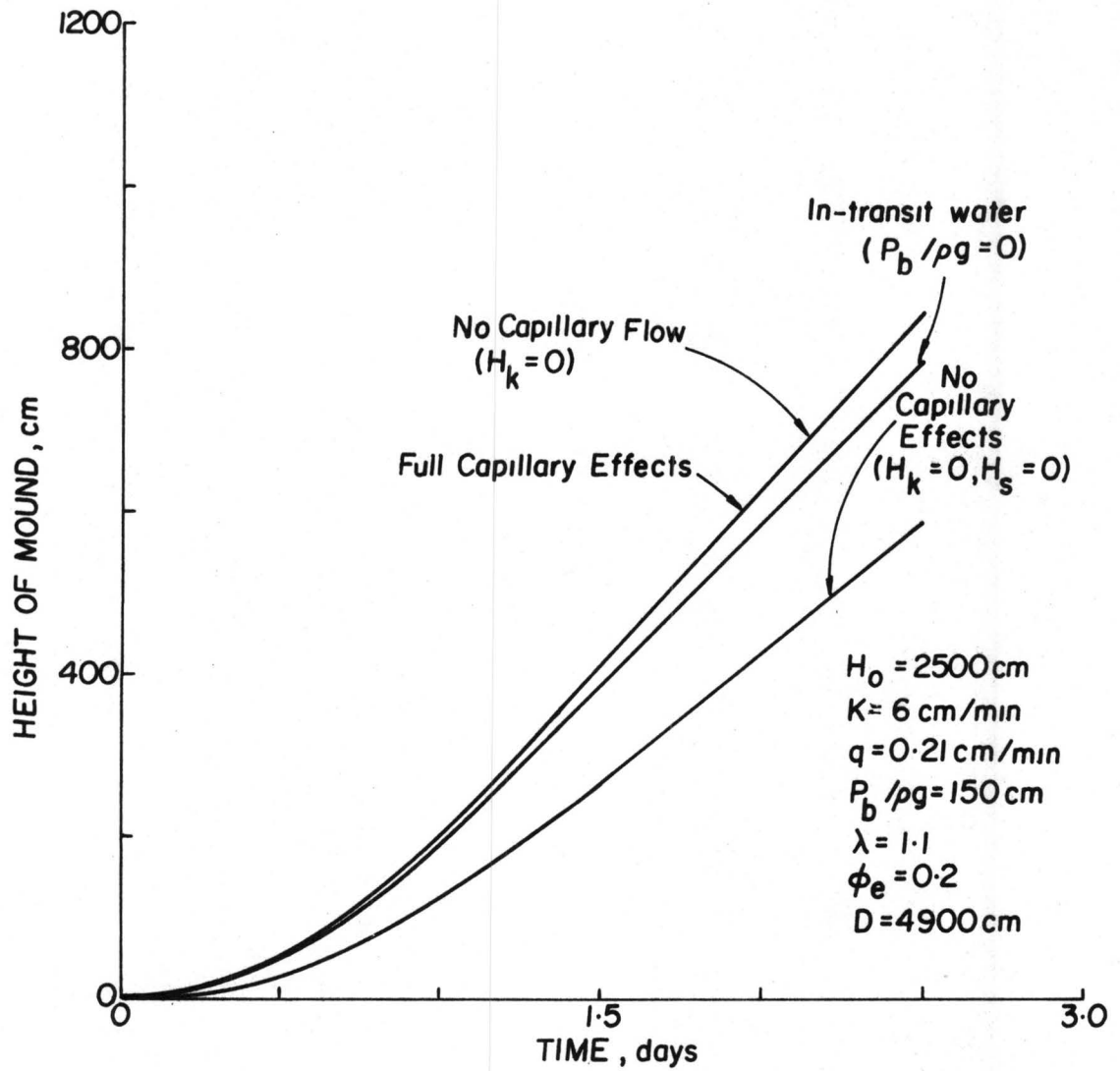


Figure 6-5. Comparison of the relative importance of capillary storage and capillary flow at 150 meters from edge recharge area.

effect of capillary storage is more important than capillary flow, the effect of capillary flow being negligible.

Since horizontal capillary flow is directly proportional to the effective permeable height, and the effective permeable height, as obtained from equation 3-10, approaches a constant at shallow water table depth, the contribution from capillary flow will be significant when the effective permeable height is of the same order of magnitude as the initial saturated thickness. In Figures 6-4 and 6-5 the effective permeable height was small compared to the total flow depth, since the initial saturated thickness was 25 meters and the bubbling pressure head was 1.5 meters. Thus, the contribution from capillary flow was expected to be negligible.

From Figure 6-4 and 6-5 it is evident that the main contribution to capillary storage is from in-transit water. Directly beneath the recharge area approximately 90 percent of the effect of capillary storage is due to the contribution from in-transit water. In the above analysis, since the depth to water table was large, the effect of the static moisture content distribution on capillary storage was small. For shallow water table depth the effect from the moisture content distribution is more pronounced since the rate of change of effective saturated height with respect to water table depth is largest. This tends to reduce the specific yield thereby resulting in larger mound heights.

It is interesting to evaluate the effects of the capillary region when the initial saturated thickness is of the same order of magnitude as the bubbling pressure head. This analysis is shown in Figures 6-6 and 6-7 for the experimental model dimensions. It is apparent that the effects of capillary storage and capillary flow are equally important.

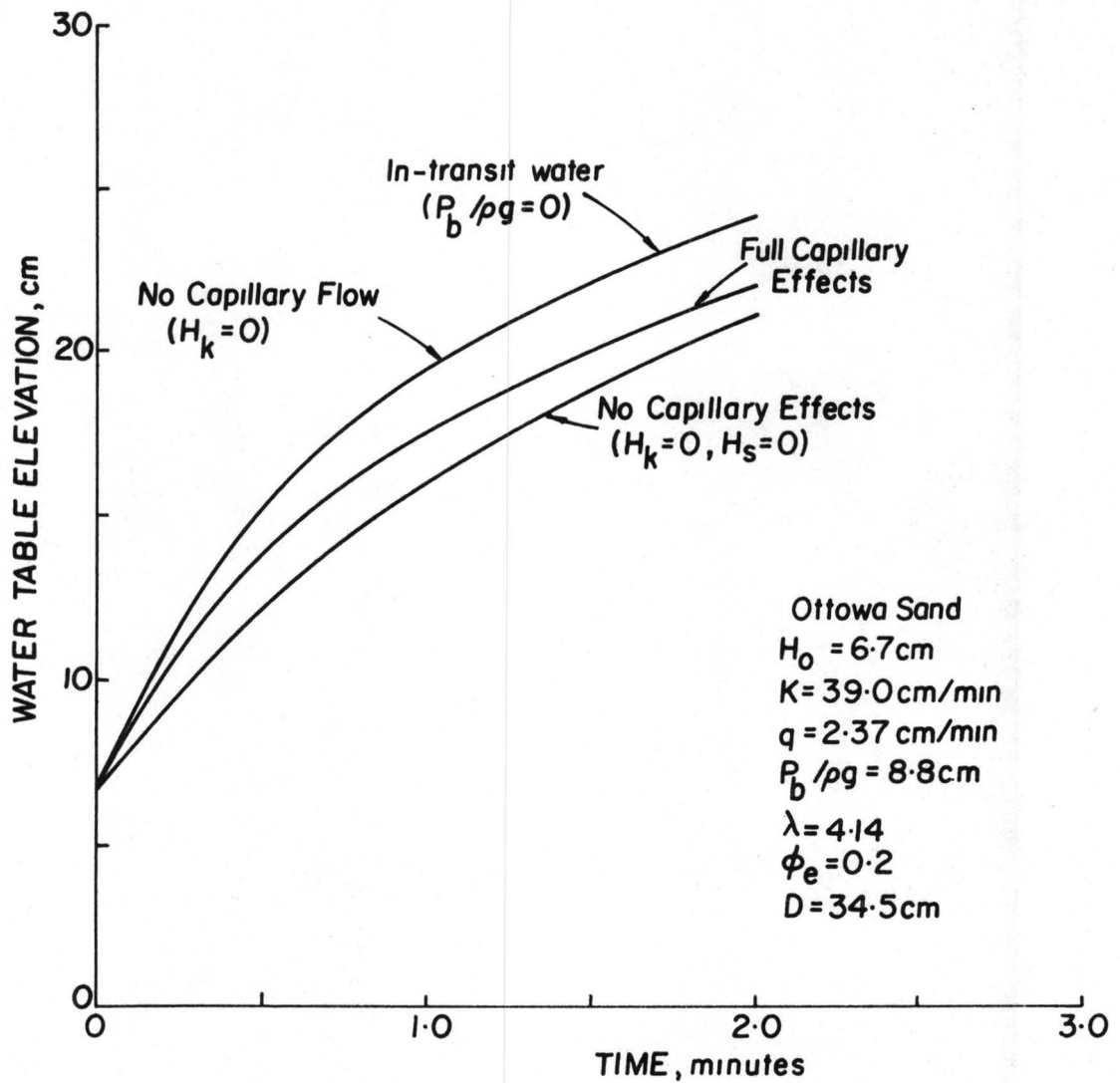


Figure 6-6. Comparison of the relative importance of capillary storage and capillary flow on central mound height.

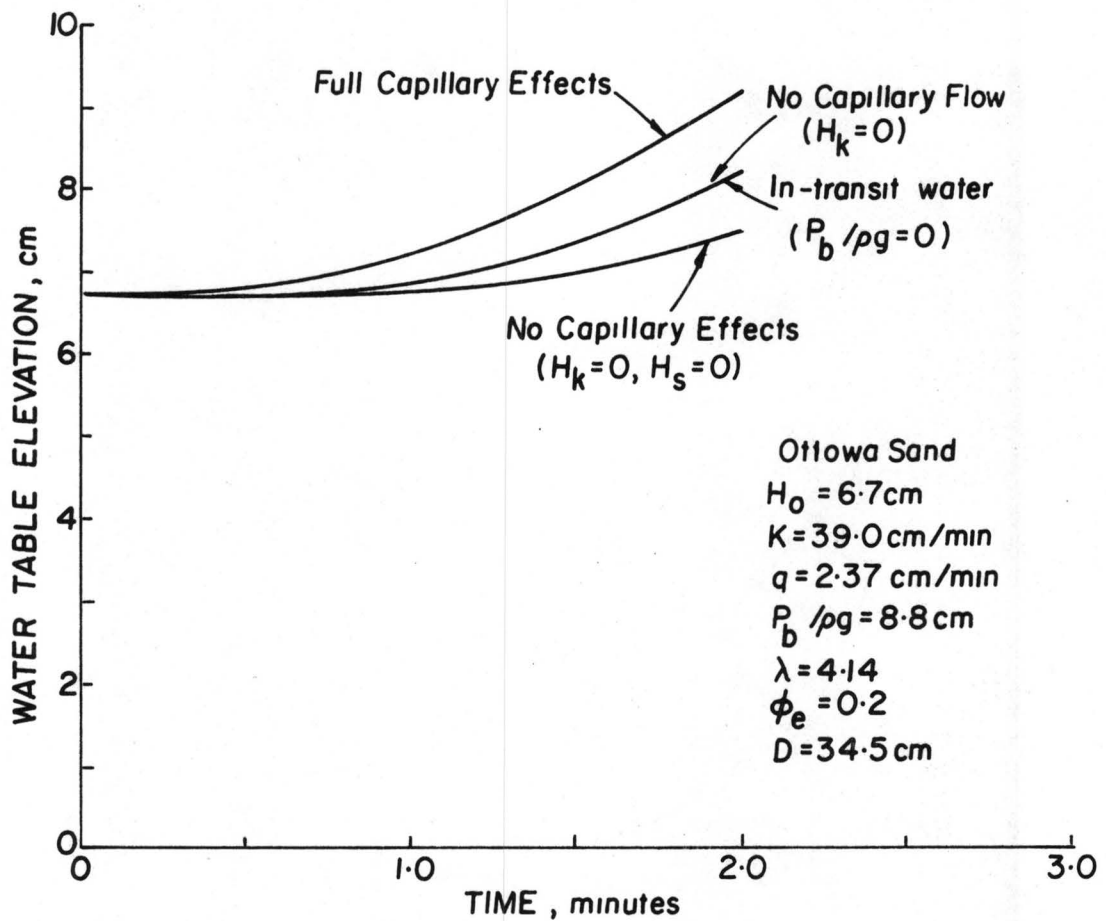


Figure 6-7. Comparison of the relative importance of capillary storage and capillary flow at 125 cm from the edge of the recharge area.

Also, the contributions to capillary storage are primarily due to in-transit water. The capillary region increases the depth through which flow can occur under no capillary conditions. This increased flow area increases the rate of flow. As a result of the increased flow rate away from the recharge area capillary flow will tend to decrease the mound heights immediately beneath the recharge site as shown in Figure 6-6. Since the horizontal gradients beneath the recharge plot are larger than away from the recharge site the rate of flow towards the toe of the mound will be greater than away from the toe of the mound. As a result an increased volume of water has to be stored beyond the recharge site thereby resulting in larger mound heights in this region. The effect of capillary flow to increase the water table depths beyond the recharge area is shown in Figure 6-7.

6.2.2 Influence of bubbling pressure head

For large saturated thickness the effect of increasing the bubbling pressure head upon the transient response of the water table to artificial recharge is shown in Figure 6-8. It is apparent that the growth of groundwater mounds beneath the recharge site is not sensitive to bubbling pressure head at least for $P_b/\rho g$ less than 8 percent of the initial saturated thickness.

Increasing the bubbling pressure head increases both the effective saturated height and the effective permeable height. This will tend to increase the effects of capillary storage and capillary flow. These effects will be significant for shallow water table depth or small initial saturated thickness or both; which was not the case considered in this analysis.

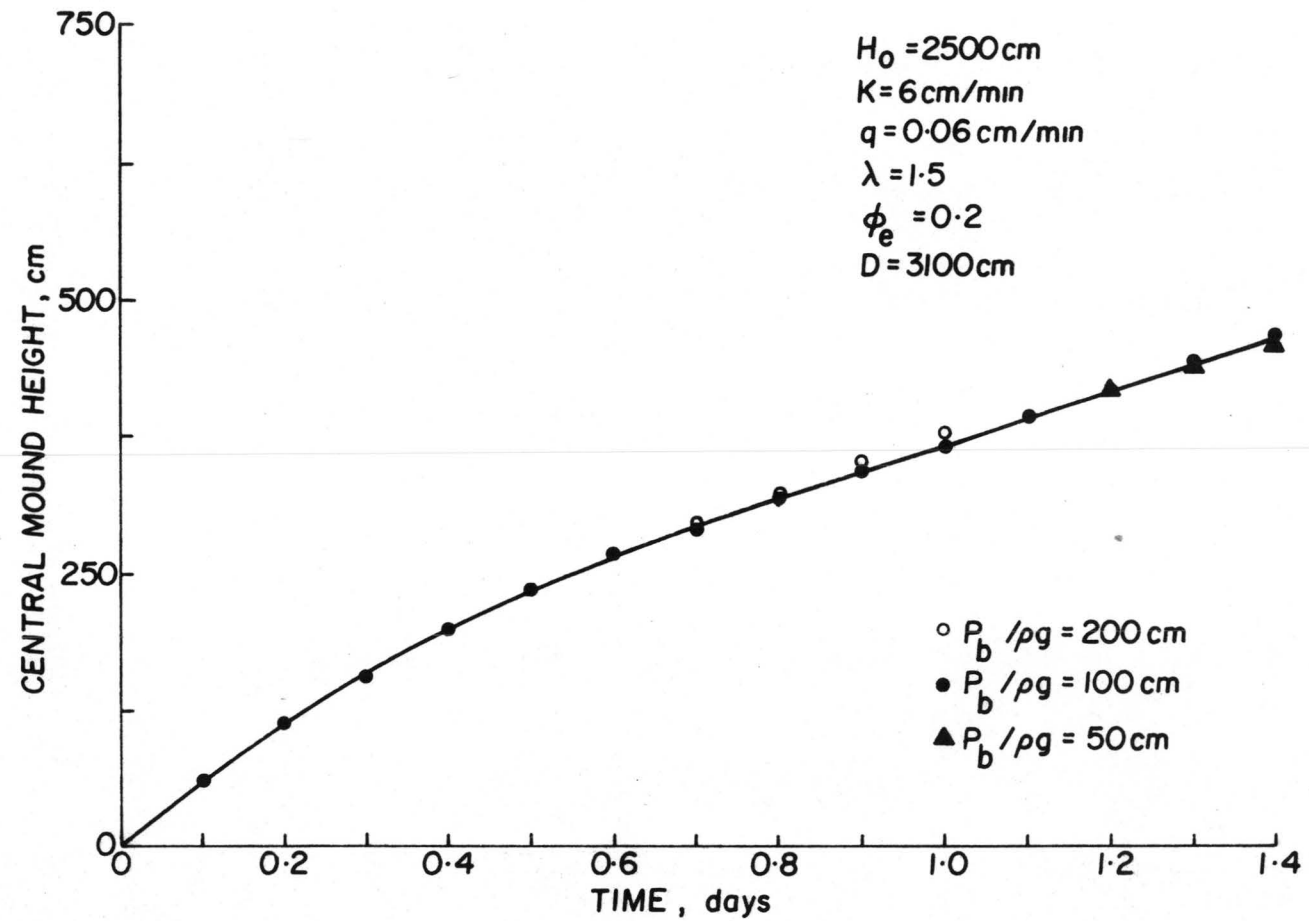


Figure 6-8. Effect of bubbling pressure head on the rate of growth of mound.

6.2.3 Influence of pore-size distribution index

The effect of decreasing the pore-size distribution index, λ , will be to increase the effective saturated height and, hence, the rate of change of the effective saturated height with respect to water table depth, thereby reducing the specific yield. As a result, the mound will rise more rapidly for smaller values of λ .

The effect of increasing λ on the central mound height is shown in Figure 6-9. It is apparent that the growth of the mound is more sensitive to λ than to the bubbling pressure head for the case analyzed. The sensitivity to changes in λ decreases as λ becomes larger.

6.2.4 Influence of initial saturated depth

It should be noted that a downward flux increases the volume of water in the partially saturated region thereby reducing the specific yield. For a larger volume of water stored in-transit, the effect of the capillary region would be greater since a smaller volume of water must move through the soil to obtain a given water table rise. On the other hand, the smaller the initial saturated thickness, the less would be the flow away from the recharge area. As a result, a larger volume of water has to be stored below the recharge site. Consequently, the effect of the capillary region on the growth of groundwater mounds would be more significant for smaller initial saturated depths.

Figure 6-10 illustrates the effect of initial saturated thickness on the development of central mound height. It can be observed that the effect of the capillary region increases as the initial saturated depth decreases. It is also apparent that the effect of the capillary region increases with time.

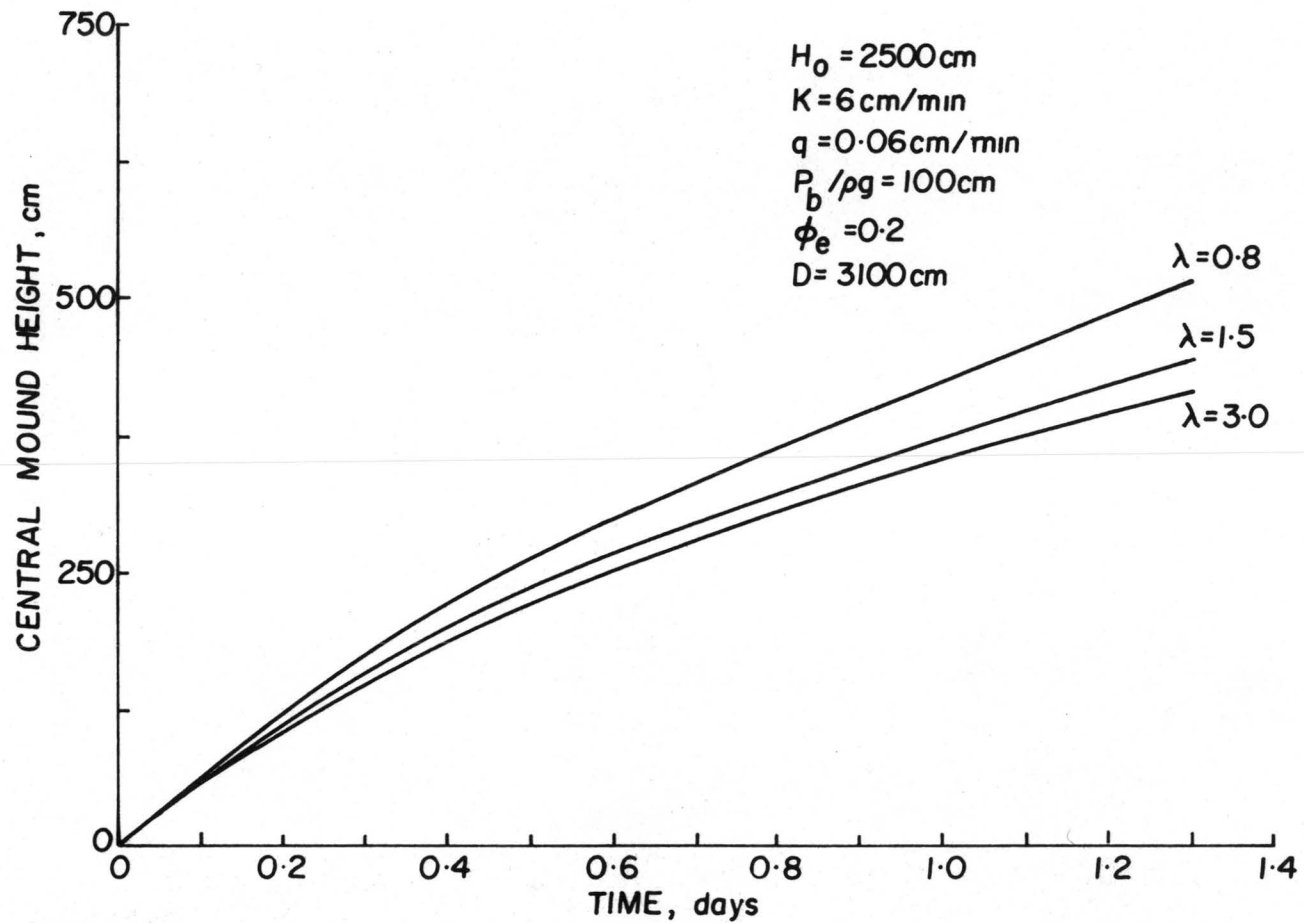


Figure 6-9. Effect of pore-size distribution index on the rate of growth of mound.

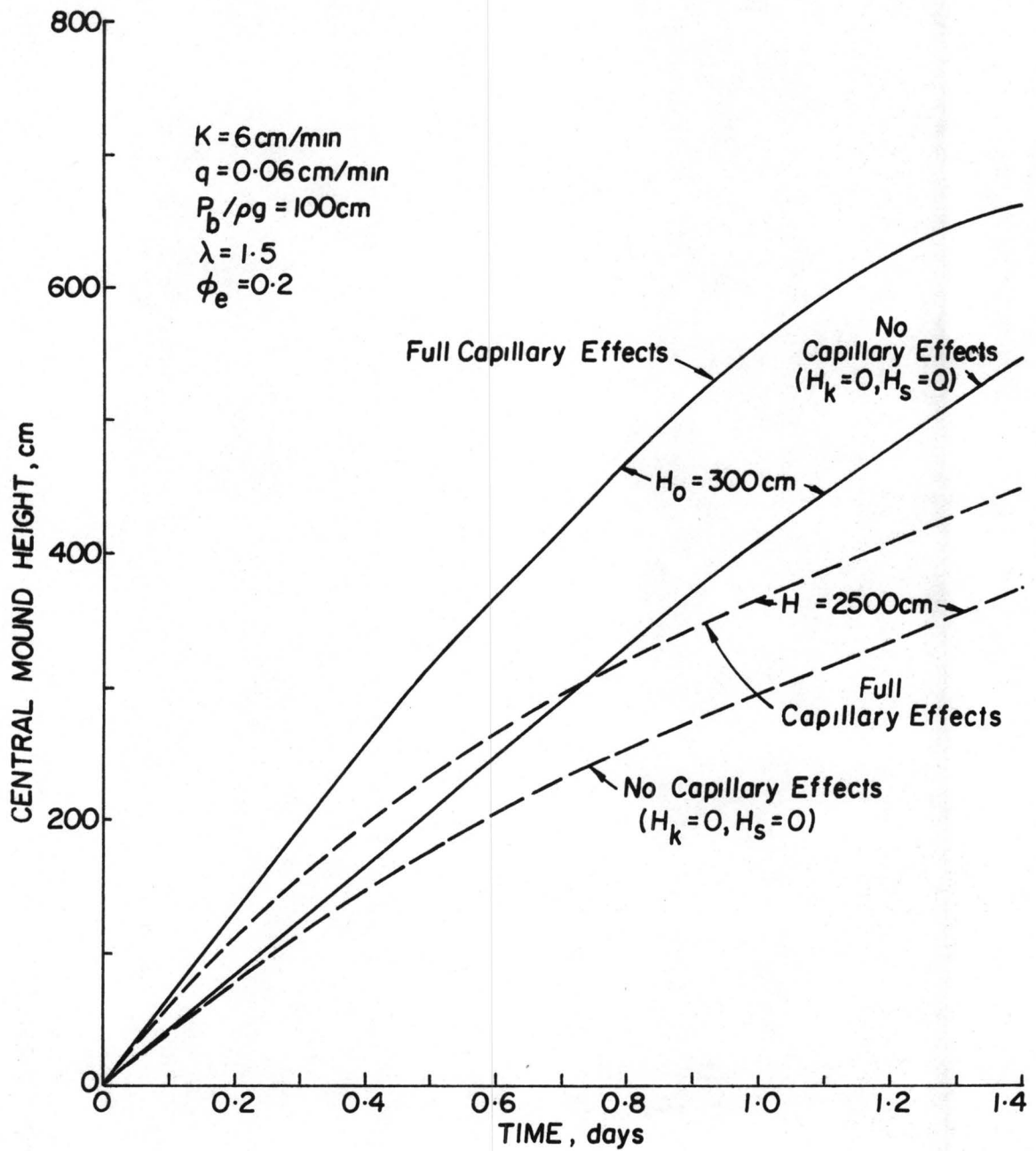


Figure 6-10. Effect of initial saturated thickness on the rate of growth of mound.

6.2.5 Influence of depth to water table

The effect of capillary storage on depth to water table is more pronounced as the water table approaches the ground surface. This water table dependence only affects the contribution from the static moisture content distribution which is very small compared to the effect of in-transit water. As a result, depth to water table will have no significant effect on central mound height, except for very shallow water table depths.

Figure 6-11 illustrates the effect of depth to water table on the transient position of the mound. It is apparent that the central mound height is not sensitive to water table depth at least for water table depths greater than 5 times the bubbling pressure head.

6.2.6 Influence of recharge rate

Since the contribution from in-transit water is more pronounced as the recharge rate is increased, the influence of capillary storage becomes more significant. As a result, the mound height obtained would be larger. The effect of scaled flux rate ($q = q/K$) upon central mound height is shown in Figure 6-12. The primary result of increased recharge is to increase the mound height. Figure 6-12 also illustrates the proportionate increase of capillary effects to increase in recharge rate.

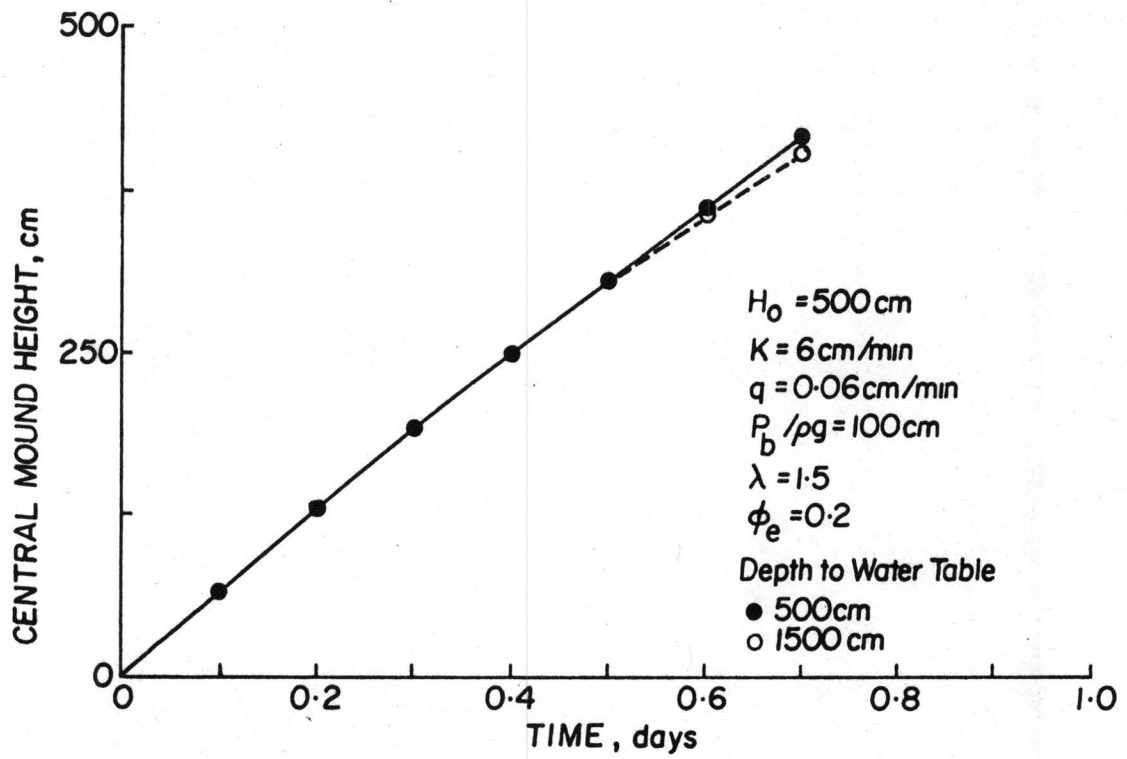


Figure 6-11. Effect of depth to water table on rate of growth of mound.

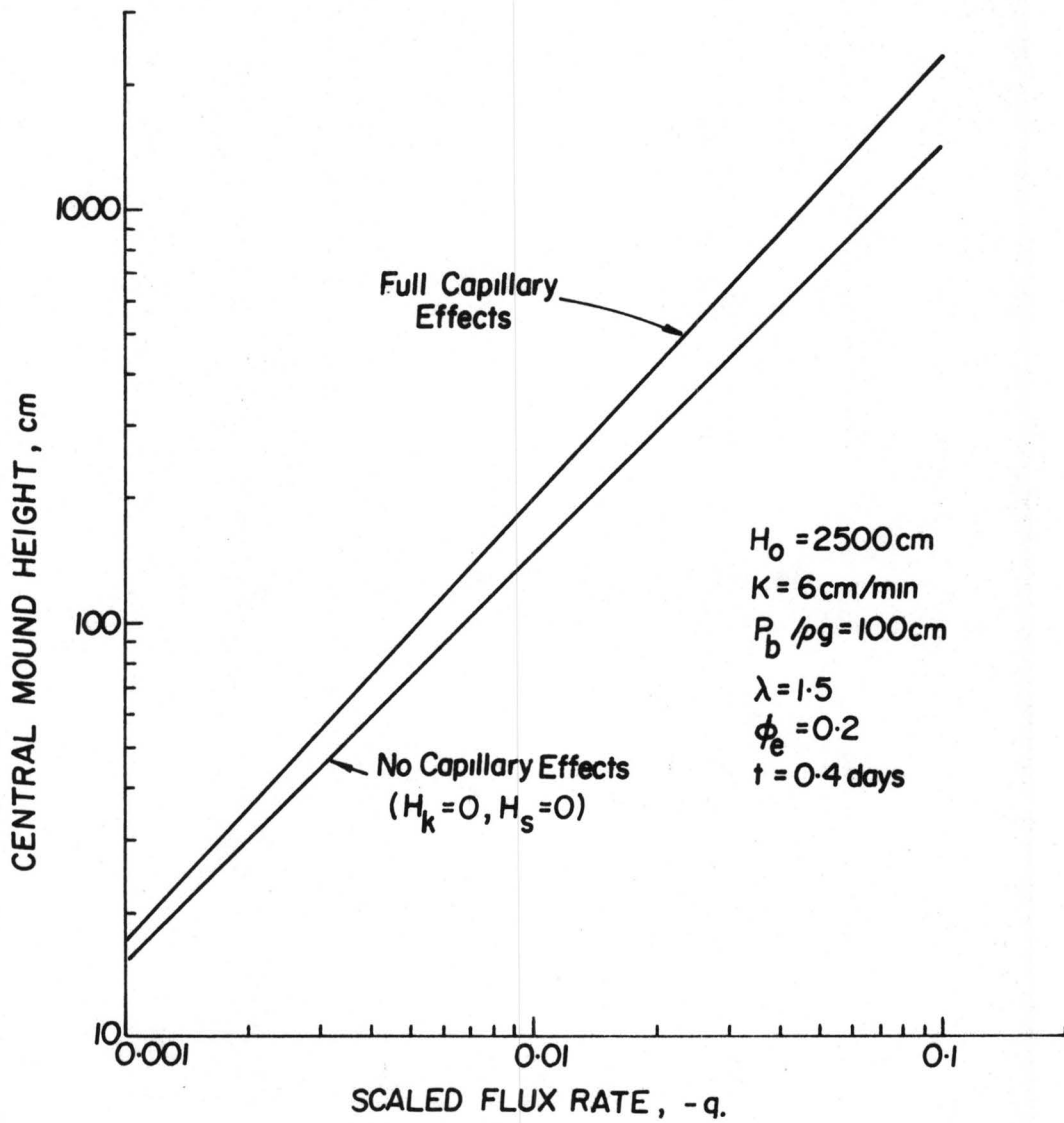


Figure 6-12. Effect of scaled flux rate on central mound height.

CHAPTER VII

SUMMARY AND CONCLUSIONS

The primary purpose of this study was to evaluate the effects of capillarity on the growth of groundwater mounds due to steady infiltration. An evaluation of the results from the physical and numerical models used in this study leads to the following conclusions.

The effects of capillarity significantly influence the development of groundwater mounds. It has been shown for the practical case analyzed that for a small rise in water table the analytical solutions underestimate the mound height by as much as 56 percent. When the rise in water table relative to the initial saturated thickness is large, previous analytical solutions do not adequately describe the growth of mounds.

The contribution from the static moisture content profile is relatively more important away from than beneath the recharge area. It has been shown that directly beneath the recharge area approximately 90 percent of the effect of capillary storage is due to the contribution from in-transit water. For ratios of initial saturated thickness to bubbling pressure head significantly greater than unity, which is the general case, capillary flow will have very little effect on the predicted mound height.

The pore-size distribution index, λ , is significantly more important than the bubbling pressure head in predicting mound heights. The sensitivity to changes in λ decreases as λ becomes larger.

Depth to water table has relatively little influence on the development of central mound height other than to limit its maximum height. For deep water tables the specific yield below the recharge area is a constant. Its magnitude depends on the recharge rate and the pore-size

distribution index. Beyond the recharge site the specific yield is equal to the drainable porosity. The effect of the capillary region on central mound height increases for decreasing initial saturated thickness and increasing recharge rate. The magnitude of the capillary effect is directly proportional to the infiltration rate.

Unless the water table is shallow and the bubbling pressure head is of the same order of magnitude as the initial saturated thickness, the hydrologist need only consider the effect of in-transit water in predicting the central mound height. Neglecting the contribution from in-transit water can lead to errors in excess of 50 percent in predicting the growth of groundwater mounds.

REFERENCES

- Arbhabhirama, A. and C. Kridkorn, Steady downward flow to a water table, Water Resources Research, 4:1968.
- Bauman, P., Groundwater movement controlled through spreading, Trans. Amer. Soc. Civil Engrs., 117:1024-1074, 1952.
- Bibby, R. and D. K. Sunada, Mathematical model of a leaky aquifer, J. of Irr. and Drain. Div., Amer. Soc. Civil Engrs., 97:IR 3:387-395, Proc. Paper 8350, 1971.
- Bittinger, M. W. and F. J. Trelease, The development and dissipation of a groundwater mound beneath a spreading basin, Amer. Soc. Agr. Engr. Trans., 15:103-106, 1965.
- Bittinger, M. W., H. R. Duke and R. A. Longenbaugh, Mathematical simulations for better aquifer management, Publ. 72 of IASH, Symposium on Artificial Recharge and Management of Aquifers, Haifa, Israel, pp. 509-519, 1967.
- Bodman, G. B. and E. A. Colman, Moisture and energy conditions during downward entry of water into soils, Proc. Soil Sci. Amer., 8:116-122, 1943.
- Bouwer, H., Theoretical aspects of flow above the water table in tile drainage of shallow homogeneous soils, Proc. Soil Sci. Soc. Amer., 23:260-263, 1959.
- Bouwer, H., Theoretical aspects of unsaturated flow in drainage and sub-irrigation, Agr. Engr., pp. 395-400, 1959.
- Bouwer, H., Unsaturated flow in groundwater hydraulics, J. of Hydr. Div. Amer. Soc. Civil Engrs., HY 5:121-144, 1964.
- Brooks, R. H. and A. T. Corey, Hydraulic properties of porous media, Colo. State Univ. Hydrology Paper No. 3, Fort Collins, 27 p., 1964.

- Chapman, T. G., Capillary effects in a two-dimensional groundwater flow system, *Geotechnique*, 10:55-61, 1960.
- Childs, E. C., A treatment of the capillary fringe in the theory of drainage, *J. Soil Sci.*, 10:83-100, 1959.
- Childs, E. C., The nonsteady state of the water table in drained land, *J. Geophys. Res.*, 65:780-782, 1960.
- Corey, G. L., A. T. Corey and R. H. Brooks, Similitude for non-steady drainage for partially saturated soil, *Colo. State Univ. Hydrology Paper No. 9*, Fort Collins, 38 p., 1965.
- Donnan, W. W., Model test of a tile spacing formula, *Proc. Soil Sci. Soc. Amer.*, 11:131-136, 1946.
- Duke, H. R., Capillary properties of soils - influence upon specific yield, *Trans. Amer. Soc. Agr. Engr.*, 688-691, 1972.
- Duke, H. R., Drainage design based upon aeration, *Colo. State Univ. Hydrology Paper No. 61*, Fort Collins, 59 p. 1973.
- Eshett, A. and R. A. Longenbaugh, Mathematical model for transient flow in porous media, *Prog. Report CER65RAL-AE59*, Civil Engr. Dept., Colo. State Univ., Fort Collins, 1965.
- Gardner, W. R., Some steady state solutions of the unsaturated moisture flow equation with application to evaporation from a water table, *Soil Sci.*, 85:228-233, 1958.
- Glass, J. P., B. A. Christensen, and H. Rubin, Analysis of transient groundwater flow from seepage ponds. For presentation at the Third International Hydrology Symposium, Fort Collins, Colo., 1977.
- Glover, R. E., Mathematical derivations as pertains to groundwater recharge, Mimeographed report, *Agr. Res. Serv., U. S. Dept. of Agr.*, Fort Collins, Colo., 118 p., 1961.

- Hanson, B. R., Entrapped gas in an unconfined aquifer, PhD Dissertation, Colo. State Univ., 111 p., 1977.
- Hantush, M. S., Growth of a groundwater ridge in response to deep percolation, Proc. Symp. Trans. Groundwater Hydraul., Fort Collins, 118 p., 1963.
- Hantush, M. S., Growth and decay of groundwater mounds in response to uniform percolation, Water Resources Research, 3:227-234, 1967.
- Hedstrom, W. E., A. T. Corey, and H. R. Duke, Models for subsurface drainage, Colo. State Univ. Hydrology Paper No. 48, Fort Collins, 56 p., 1971.
- Laliberte, G. E., A. T. Corey and R. H. Brooks, Properties of porous media, Colo. State Univ. Hydrology Paper No. 17, Fort Collins, 1966.
- Luthin, J. N. and R. V. Worstell, The falling water table in tile drainage - I. A laboratory study, Proc. Soil Sci. Soc., Amer., 21:580-584, 1957.
- Luthin, J. N., The falling water table in tile drainage - II. Proposed criteria for spacing tile drains, Trans. Amer. Soc. Agr. Engrs., 2:44-45, 1959.
- Marino, M. A., Growth and decay of groundwater mounds induced by percolation, J. of Hydrol., 22:295-301, 1974.
- Marmion, K. R., Hydraulics of artificial recharge in nonhomogeneous formations, Hydraulic Lab., Univ. of Calif., Berkeley, 88 p., 1962.
- Schilfgaarde, J. van, Theory of flow to drains, Advanc. Hydrosoci., 6: 43-106, 1970.
- Schmid, P. and J. Luthin, The drainage of sloping lands, J. Geophys. Res., 69:1525-1529, 1964.

Smith, R. E., Mathematical simulation of infiltrating watersheds, PhD Dissertation, Colo. State Univ., 193 p., 1970.

White, N. F., D. K. Sunada, H. R. Duke and A. T. Corey, Boundary effects in desaturation of porous media, Soil Sci., 113:7-13, 1972.

Youngs, E. G., Hodograph solution of the drainage problem with very small drain diameter, Water Resources Research, 6:594-600, 1970.

APPENDIX A

DESCRIPTION OF PROGRAM RECAP1

Program RECAP1 consists of a main controlling program and several subprograms. The main program's function is to control the execution of subroutines for all time steps at which calculations are desired. The subprograms are designed for specific tasks, such as physical parameter input, effective height computations and solving a set of simultaneous equations. A description of each subprogram, boundary and initial conditions, selection of time increment and a listing of the computer program RECAP1 are presented in this section.

A-1 Boundary and Initial Conditions

Boundary conditions due to geologic and hydrologic influences include (1) impermeable or no flow boundaries, (2) constant head boundaries, and (3) constant gradient boundaries. This program utilizes an initial water level coding to distinguish the type of boundary. $H(I,J)$ is the initial water level in grid I,J and the coding used is:

- $0 < H(I,J) < 10,000$ - actual water level elevation,
- $10,000 \leq H(I,J) < 20,000$ - impermeable grid,
- $20,000 \leq H(I,J) < 30,000$ - constant gradient grid,
- $30,000 \leq H(I,J) < 40,000$ - constant head grid.

For each case presented in this study the initial condition is that of a horizontal water table and the boundary conditions were either impermeable or constant head.

A-2 Selection of Time Increment

The maximum size of time increment, DT , which will provide adequate accuracy should be used to conserve computer time. The optimum DT was determined by performing short period analyses with varying DT values

for the selected grid dimensions. Smaller grid dimensions may require shorter time increments. The number of rows (NR) should always be less than the number of columns (NC) to conserve computer time during the solution of the set of simultaneous equations.

A-3 Description of Subprograms

Subroutine READPH

This subroutine reads and writes the physical data describing the study area. The following variables are read and printed: DX, DY, FK, Z, Q, PHI, D, SLMD, BUBPH and QDOT. Q must be read in matrix form. Variables DX and DY require only NC and NR respectively. For each case presented the aquifer was assumed to be resting on a horizontal impermeable base and the hydraulic conductivity was uniform for each grid. Therefore, only one data card is required to enter the remaining parameters.

Called from: Main Program

Subprograms used: MATROP

Important variables: DX, DY, FK, Z, Q, PHI, D, SLMD, BUBPH, QDOT.

Subroutine READH

This subroutine reads the initial coded water table elevations. H is decoded and set equal to HT and HP. One data card is required for a horizontal water table.

Called from: Main Program

Subprograms used: None

Important variables: H, HT, HP.

Subroutine MATSOL

This subroutine sets up the coefficient matrix, CMATRX, and the right hand side vector matrix, CR. CMATRX is a reduced matrix containing

only the band of known values in the left side of the difference equations and is written vertically rather than diagonally. Its dimensions are $(NR-2)*(NC-2)$ by $2*(NR-3)$. The coefficients are computed using Function PARAM and checked for adjacent boundary values of H in subroutine NSCOUNT. MATSOL treats known grid values of H. BSOLVE is used to solve the matrix equation set up.

Called from: Main Program

Subprograms used: PARAM, NSCOUNT, BSOLVE

Important variables: CMATRX, CR.

Subroutine NSCOUNT

This subroutine transfers the coefficients, in CMATRX, multiplied by their respective H-value, to the right hand side vector matrix in case of constant head or known boundary conditions. It also sets coefficients equal to zero in case of impermeable boundaries.

Called from: MATSOL

Subprograms used: None

Important variables: None.

Subroutine BSOLVE

This subroutine solves the matrix equation set up in MATSOL by Gauss Elimination. BSOLVE is designed specifically for a diagonal matrix that results from analysis of groundwater systems.

Called from: MATSOL

Subprograms used: None

Important variables: None.

Subroutine ESATHS

This subroutine evaluates the effective saturated height and the effective permeable height as a function of elevation when the

infiltration rate is zero.

Called from: Main Program

Subprograms used: None

Important variables: HSQO, HKQO, SLMD, BUBPH, PETA.

Subroutine ESATHQ

This subroutine evaluates the effective saturated height as a function of elevation when the infiltration rate is greater than zero. Integrals are evaluated by Gaussian quadrature.

Called from: Main Program

Subprograms used: None

Important variables: HS, SLMD, PETA, BUBPH, QDOT.

Subroutine SPYLD

This subroutine computes the specific yield.

Called from: Main Program

Subprograms used: None

Important variables: HS, HSQO, HT, HP, SY, D, PHI.

Subroutine EFL0D

This subroutine evaluates the total depth available for horizontal flow. This depth of horizontal flow is the sum of the water table height and the effective permeable height calculated from ESATHS.

Called from: Main Program

Subprograms used: None

Important variables: HP, HKQO, HF, D.

Subroutine MATROP

This subroutine organizes data or results into a suitable form for printing and then prints.

Called from: Main Program, READPH, READH

Subroutines used: None

Important variables: NR, NC.

Function PARAM

This subprogram computes the coefficients in the left side of the finite-difference equation.

Called from: MATSOL

Subprograms used: None

Important variables: PARAM.

A-4 Program Listing

On the following pages is the listing of the program RECAP1.

PROGRAM RECAP1

```

PROGRAM RECAP1
1 (INPUT,OUTPUT,TAPES=INPUT,TAPE6=OUTPUT)

C
C EVALUATE TRANSIENT RESPONSE OF THE WATER TABLE TO ARTIFICIAL
C RECHARGE,BASED ON DUPUIT-FORCHHEIMER ASSUMPTIONS,CONSIDERING FLOW
C AND STORAGE IN THE CAPILLARY REGION.
C
C N. ORTIZ JUNE 1977, CDC 6400
C
C
C DIMENSION
C 1 DX(5,16) , FK(5,16) , SY(5,16) , Z(5,16) ,
C 2 HP(5,16) , O(5,16) , H(5,16) , HT(5,16) ,
C 3 DIBT(16) , DILT(5) , DITP(16) , DIRT(5) ,
C 4 HS(2500) , HSGO(2500) , CMATRX(42,7) , CR(42) ,
C WRITE (6,220)
C READ (5,230) NC,NP,LOOPUL,OT,NOP
C WRITE (6,230) NC,NP,LOOPUL,OT
C
C CONTROL VARIABLES
C NC=NUMBER OF COLUMNS(DIMENSIONLESS)
C NR=NUMBER OF ROWS (DIMENSIONLESS)
C NR SHOULD ALWAYS BE LESS THAN OR EQUAL TO NC
C LOOPUL=NUMBER OF TIME STEPS(DIMENSIONLESS)
C DT=TIME INCREMENT(T)
C
C ARRAY NAMES DEFINED AS FOLLOWS.
C FK-SATURATED HYDRAULIC CONDUCTIVITY (L/T)
C SY-SPECIFIC YIELD (DIMENSIONLESS)
C Z-BEDROCK ELEVATION (L)
C DX-X-DIMENSION OF GRID (L)
C DY-Y-DIMENSION OF GRID (L)
C H-INITIAL WATER TABLE ELEVATION (L)
C HT-PRESENT WATER TABLE ELEVATION (L)
C HP-WATER TABLE ELEVATION AT PREVIOUS TIME LEVEL (L)
C Q-NET SURFACE INFLOW PER GRID -POSITIVE DOWNWARDS(V/T)
C DITP-GRADIENT TOP BOUNDARY-CONSTANT GRADIENT BOUNDARY ONLY(L)
C DIRT-GRADIENT RIGHT BOUNDARY-CONSTANT GRADIENT BOUNDARY ONLY(L)
C DIBT-GRADIENT BOTTOM BOUNDARY-CONSTANT GRADIENT BOUNDARY ONLY(L)
C DILT-GRADIENT LEFT BOUNDARY-CONSTANT GRADIENT BOUNDARY ONLY(L)
C CMATRX-ELEMENTS OF THE COEFFICIENT MATRIX
C CR-ELEMENTS OF THE RIGHT HAND SIDE VECTOR MATRIX
C HS-EFFECTIVE SATURATED HEIGHT AS A FUNCTION OF ELEVATION-
C INFILTRATION PRESENT(L)
C HSGO-EFFECTIVE SATURATED HEIGHT AS A FUNCTION OF ELEVATION-
C NO INFILTRATION(L)
C HKGO-EFFECTIVE PERMEABLE HEIGHT AS A FUNCTION OF ELEVATION-
C NO INFILTRATION(L)
C HF-TOTAL DEPTH AVAILABLE FOR HORIZONTAL FLOW(L)
C
C NOP=CAPILLARY OPTIONS
C 0=FULL CAPILLARY EFFECTS
C 1=INTRASIT WATER
C 2=NO CAPILLARY FLOW
C 3=NO CAPILLARY EFFECTS
C 4=NO CAPILLARY STORAGE
C
C CALL READH (NR,NC,H,HP,HT,HM)
C CALL READPH (NR,NC,FK,SY,Z,DX,DY,HF,PHI,D,SLMD,BURPH,QDOT,Q,PETA)
C N = (U - HM + 1.0)
C IF ((NOP.EQ.1).OR.(NOP.EQ.3)) BURPH = 0.00001
C
C CALCULATE EFFECTIVE PERMEABLE HEIGHT AND EFFECTIVE SATURATED
C HEIGHT WHEN INFILTRATION RATE IS ZERO.
C
C CALL ESATHS (SLMD,BURPH,HSGO,HKGO,PETA,N)
C
C CALCULATE EFFECTIVE SATURATED HEIGHT WHEN INFILTRATION RATE IS
C GREATER THAN ZERO.
C
C CALL ESATHQ (SLMD,PETA,BURPH,HS,QDOT,N)
C IF (NOP.LT.3) GO TO 110
C DO 100 I = 1,NR
C DO 100 J = 1,NC
C SY(I,J) = PHT
C 100 CONTINUE

```

```

110 CONTINUE
DO 210 I5 = 1, LOOPUL
  IT1 = MOD(I5, 1)
  T = DT * I5
C
C   NA AND NB DETERMINE THE SIZE OF THE REDUCED BAND MATRIX.
C
  NA = (NR - 2) * (NC - 2)
  NB = 2 * NR - 3
  ICD = 2 * NR - 3
  IRD = (NR - 2) * (NC - 2)
C
C   CALCULATE SPECIFIC YIELD
C
  IF (NOP.GT.2) GO TO 120
  CALL SPYLD (HS, HSQ0, HT, HP, SY, NC, NR, D, PHI, I5, 1, 200T, SLMD, PETA)
120 CONTINUE
  IF (IT1.EQ.0) WRITE (6, 240) T
  IF (IT1.EQ.0) CALL MATROP (NR, NC, SY)
  DO 130 I = 1, NR
    DO 130 J = 1, NC
      HP(I, J) = HT(I, J)
130 CONTINUE
  IF ((NOP.EQ.0).OR.(NOP.EQ.4)) GO TO 150
  DO 140 I = 1, NR
    DO 140 J = 1, NC
      HF(I, J) = HP(I, J)
140 CONTINUE
150 CONTINUE
C
C   CALCULATE THE DEPTH AVAILABLE FOR HORIZONTAL FLOW.
C
  IF ((NOP.GE.1).AND.(NOP.LE.3)) GO TO 160
  CALL EFLOD (HP, HKQ0, HF, NR, NC, D, N)
160 CONTINUE
  IF (IT1.EQ.0) WRITE (6, 250) T
  IF (IT1.EQ.0) CALL MATROP (NR, NC, HF)
  CALL MATSOL (NR, NC, NA, NB, FK, SY, H, HT, Z, DX, DY, 1, DT, IRD, ICC, CMATRX
1, CR, HF)
  NR1 = NR - 1
  NC1 = NC - 1
C
C   DO 4 AND DO 5 LOOPS ADJUST THE BOUNDARY ELEVATIONS H(I, J) FOR THE
C
  DO 180 I2 = 2, NC1
    IF (H(I1, I2).GE.30000.0) GO TO 170
    HT(I1, I2) = HT(I2, I2) + DITP(I2)
    IF (H(I1, I2).GE.20000.0) GO TO 170
    HT(I1, I2) = H(I1, I2)
170 IF (H(NR, I2).GE.30000.0) GO TO 180
    HT(NR, I2) = HT(NR1, I2) - DIBT(I2)
    IF (H(NR, I2).GE.20000.0) GO TO 180
    HT(NR, I2) = H(NR, I2)
180 CONTINUE
  DO 200 I1 = 2, NR1
    IF (H(I1, 1).GE.30000.0) GO TO 190
    HT(I1, 1) = HT(I1, 2) + DITP(I1)
    IF (H(I1, 1).GE.20000.0) GO TO 190
    HT(I1, 1) = H(I1, 1)
190 IF (H(I1, NC).GE.30000.0) GO TO 210
    HT(I1, NC) = HT(I1, NC1) - DIBT(I1)
    IF (H(I1, NC).GE.20000.0) GO TO 210
    HT(I1, NC) = H(I1, NC)
200 CONTINUE
  IF (IT1.EQ.0) WRITE (6, 260) T
  IF (IT1.EQ.0) CALL MATROP (NR, NC, HT)
210 CONTINUE
  STOP
C
220 FORMAT (3X, 2HNC, 4X, 2HNR, 1X, 6HLCOPUL, 1X, 4HDELTA)
230 FORMAT (3I5, F10.4, I10)
240 FORMAT (50X, 25HSPECIFIC YIELD MAP AT T =, F7.0, 1X, 7HMINUTES)
250 FORMAT (50X, 42HDEPTH AVAILABLE FOR HORIZONTAL FLOW AT T =, F7.0
1, 1X, 7HMINUTES)
260 FORMAT (50X, 22HWATER LEVEL MAP AT T =, F7.0, 1X, 7HMINUTES)
END

```

A 0075
A 0076
A 0077
A 0078
A 0079
A 0080
A 0081
A 0082
A 0083
A 0084
A 0085
A 0086
A 0087
A 0088
A 0089
A 0090
A 0091
A 0092
A 0093
A 0094
A 0095
A 0096
A 0097
A 0098
A 0099
A 0100
A 0101
A 0102
A 0103
A 0104
A 0105
A 0106
A 0107
A 0108
A 0109
A 0110
A 0111
A 0112
A 0113
A 0114
A 0115
A 0116
A 0117
A 0118
A 0119
A 0120
A 0121
A 0122
A 0123
A 0124
A 0125
A 0126
A 0127
A 0128
A 0129
A 0130
A 0131
A 0132
A 0133
A 0134
A 0135
A 0136
A 0137
A 0138
A 0139
A 0140
A 0141
A 0142
A 0143
A 0144
A 0145
A 0146
A 0147
A 0148
A 0149
A 0150

SUBROUTINE MATSOL

```

SUBROUTINE MATSOL (NOROW,NOCOL,IP,IR,FK,SV,H,HT,Z,DELX,DELY,Q,DELT  B 0002
1,IPD,ICD,CMATRX,CR,HF)  B 0003
DIMENSION  FKN(NOROW,NOCOL) , SY(NOROW,NOCOL),  B 0004
1 H(NOROW,NOCOL) , HT(NOROW,NOCOL) ,  B 0005
2 Z(NOROW,NOCOL) , DELX(NOROW,NOCOL) ,  B 0006
3 DELY(NOROW,NOCOL) , Q(NOROW,NOCOL) ,  B 0007
4 CMATRX(IPD,ICD) , CR(IPD) , HF(NOROW,NOCOL)  B 0008
C  B 0009
C DIMENSION FOR CMATRX((NR-2)*(NC-2),2*NR-3) AND FOR CR((NR-2)*(NC-  B 0010
C THIS SUBROUTINE SETS UP THE COEFFICIENT MATRIX AND THE RIGHT HAND  B 0011
C MATRIX  B 0012
C THE COEFFICIENTS ARE COMPUTED BY THE FUNCTION PARAM. THE FORMULA U  B 0013
C IN PARAM IS APPLICABLE TO CASES WITH VARIABLE DY, DX, FK, AND SATU  B 0014
C THICKNESS  B 0015
C CMATRX - ELEMENTS OF THE COEFFICIENT MATRIX  B 0016
C CR - ELEMENTS OF THE RIGHT HAND SIDE VECTOR MATRIX  B 0017
C THE MATRIX OBTAINED HAS ITS ZERO COLUMNS ELIMINATED.  B 0018
C  B 0019
PARAM(AK1,AK2,AH1,AH2,AZ1,AZ2,AX1,AX2,AY1,AY2) = (2. * AK1 * AK2 *  B 0020
1 AY1 * AY2 * (AMAX1(AH1,AH2) - AMAX1(AZ1,AZ2)))/(AX1 * AK2 * AY2)  B 0021
2 + (AX2 * AK1 * AY1))  B 0022
DO 100 J = 1,IR  B 0023
DO 100 I = 1,IP  B 0024
100 CMATRX(I,J) = 0.0  B 0025
NT = 0  B 0026
NC1 = NOCOL - 1  B 0027
NR1 = NOROW - 1  B 0028
IB = NOROW - 2  B 0029
IM = IB + 1  B 0030
IC = IM + 1  B 0031
IO = 2 * IB + 1  B 0032
DO 120 J = 2,NC1  B 0033
DO 120 I = 2,NR1  B 0034
NT = NT + 1  B 0035
CR(NT) = 0.0  B 0036
IF (H(I,J).GE.10000.0) GO TO 110  B 0037
JA = I  B 0038
JD = I  B 0039
CMATRX(NT,1) = PARAM(FK(JA,J - 1),FK(I,J),HF(JA,J - 1),HF(I,J),  B 0040
1 Z(JA,J - 1),Z(I,J),DELX(JA,J - 1),DELY(JA,J - 1),DELT  B 0041
2 (I,J))  B 0042
CMATRX(NT,IB) = PARAM(FK(I - 1,J),FK(I,J),HF(I - 1,J),HF(I,J),Z  B 0043
1 (I - 1,J),Z(I,J),DELY(I - 1,J),DELY(I,J),DELX(I - 1,J),DELX(I,J)  B 0044
2 ))  B 0045
CMATRX(NT,IC) = PARAM(FK(I + 1,J),FK(I,J),HF(I + 1,J),HF(I,J),Z  B 0046
1 (I + 1,J),Z(I,J),DELY(I + 1,J),DELY(I,J),DELX(I + 1,J),DELX(I,J)  B 0047
2 ))  B 0048
CMATRX(NT,IO) = PARAM(FK(JD,J + 1),FK(I,J),HF(JD,J + 1),HF(I,J)  B 0049
1 ,Z(JD,J + 1),Z(I,J),DELX(JD,J + 1),DELY(JD,J + 1),DELT  B 0050
2 Y(I,J))  B 0051
CALL NSCONT (H(JA,J - 1),HT(JA,J - 1),HT(I,J),Z(JA,J - 1),Z(I,J)  B 0052
1 ),CMATRX(NT,1),CMATRX(NT,IM),CR(NT))  B 0053
CALL NSCONT (H(I - 1,J),HT(I - 1,J),HT(I,J),Z(I - 1,J),Z(I,J),C  B 0054
1 MATRX(NT,IB),CMATRX(NT,1),CR(NT))  B 0055
CALL NSCONT (H(I + 1,J),HT(I + 1,J),HT(I,J),Z(I + 1,J),Z(I,J),C  B 0056
1 MATRX(NT,IC),CMATRX(NT,IM),CR(NT))  B 0057
CALL NSCONT (H(JD,J + 1),HT(JD,J + 1),HT(I,J),Z(JD,J + 1),Z(I,J)  B 0058
1 ),CMATRX(NT,IO),CMATRX(NT,IM),CR(NT))  B 0059
CMATRX(NT,IM) = CMATRX(NT,IM) - (CMATRX(NT,1) + CMATRX(NT,IB) +  B 0060
1 CMATRX(NT,IC) + CMATRX(NT,IO) + (SY(I,J) * DELX(I,J) * DELY(I,  B 0061
2 J))/DELT)  B 0062
CR(NT) = CR(NT) - (HT(I,J) * SY(I,J) * DELX(I,J) * DELY(I,J))/D  B 0063
1 ELT - Q(I,J)  B 0064
GO TO 120  B 0065
110 CMATRX(NT,IM) = 1.0  B 0066
CR(NT) = HT(I,J)  B 0067
120 CONTINUE  B 0068
CALL BSOLVE (CMATRX,IP,IR,CR)  B 0069
NT = 0  B 0070
DO 130 J = 2,NC1  B 0071
DO 130 I = 2,NR1  B 0072
NT = NT + 1  B 0073
130 HT(I,J) = CR(NT)  B 0074
RETURN  B 0075
END  B 0076

```


SUBROUTINE NSCONT

```

C      SUBROUTINE NSCONT (HA,HTA,HTM,ZA,ZM,CRXA,CRXM,CRL)
C
C      THIS SUBROUTINE TRANSFERS THE COEFFICIENTS, MULTIPLIED BY THEIR RE
C      H-VALUE, TO THE RIGHT HAND SIDE VECTOR MATRIX IN CASE OF CONSTANT
C      KNOWN BOUNDARY CONDITIONS. IT ALSO SETS COEFFICIENTS EQUAL TO ZERO
C      OF IMPERMEABLE BOUNDARIES.
C
C      IF (HA.LT.20000.0) GO TO 100
C      CRL = CRL - CRXA * HTA
C      CRXM = CRXM - CRXA
C      CRXA = 0.0
C      GO TO 110
100 IF (HA.GE.10000.0) GO TO 120
110 IF ((HTM - ZM).LE.1.0.AND.HTM.GT.HTA) GO TO 120
    IF ((HTA - ZA).GT.1.0.OR.HTA.LE.HTM) GO TO 130
120 CRXA = 0.0
130 RETURN
    END

```

C 0002
 C 0003
 C 0004
 C 0005
 C 0006
 C 0007
 C 0008
 C 0009
 C 0010
 C 0011
 C 0012
 C 0013
 C 0014
 C 0015
 C 0016
 C 0017
 C 0018
 C 0019

SUBROUTINE BSOLVE

```

C      SUBROUTINE BSOLVE (C,N,M,V)
C
C      THIS SUBROUTINE SOLVES THE MATRIX, SET UP IN MATSOL, BY GAUSS ELIM
C
C      DIMENSION      C(N,M)      , V(N)
C      LR = (M - 1)/2
C      DO 110 L = 1,LR
C      IM = LR - L + 1
C      DO 110 I = 1,IM
C      DO 100 J = 2,M
C      C(L,J - 1) = C(L,J)
C      KN = N - L
C      KP = M - I
C      C(L,M) = 0.0
100 C(KN + 1,KP + 1) = 0.0
    LR = LR + 1
    IM = N - 1
    DO 140 I = 1,IM
      NPIV = I
      LS = I + 1
      DO 120 L = LS,LR
        IF (ABS(C(L,1)).GT.ABS(C(NPIV,1))) NPIV = L
120 CONTINUE
        IF (NPIV.LE.I) GO TO 140
        DO 130 J = 1,M
          TEMP = C(I,J)
          C(I,J) = C(NPIV,J)
130 C(NPIV,J) = TEMP
          TEMP = V(I)
          V(I) = V(NPIV)
          V(NPIV) = TEMP
140 V(I) = V(I)/C(I,1)
        DO 150 J = 2,M
          C(I,J) = C(I,J)/C(I,1)
150 DO 170 L = LS,LR
          TEMP = C(L,1)
          V(L) = V(L) - TEMP * V(I)
          DO 160 J = 2,M
            C(L,J - 1) = C(L,J) - TEMP * C(I,J)
160 C(L,M) = 0.0
          IF (LR.LT.M) LR = LR + 1
170 CONTINUE
          V(N) = V(N)/C(N,1)
          JM = 2
          DO 200 I = 1,IM
            L = N - I
            DO 190 J = 2,JM
              KM = L + J
190 V(L) = V(L) - C(L,J) * V(KM - 1)
              IF (JM.LT.M) JM = JM + 1
200 CONTINUE
    RETURN
    END

```

D 0002
 D 0003
 D 0004
 D 0005
 D 0006
 D 0007
 D 0008
 D 0009
 D 0010
 D 0011
 D 0012
 D 0013
 D 0014
 D 0015
 D 0016
 D 0017
 D 0018
 D 0019
 D 0020
 D 0021
 D 0022
 D 0023
 D 0024
 D 0025
 D 0026
 D 0027
 D 0028
 D 0029
 D 0030
 D 0031
 D 0032
 D 0033
 D 0034
 D 0035
 D 0036
 D 0037
 D 0038
 D 0039
 D 0040
 D 0041
 D 0042
 D 0043
 D 0044
 D 0045
 D 0046
 D 0047
 D 0048
 D 0049
 D 0050
 D 0051
 D 0052
 D 0053
 D 0054

SUBROUTINE READH

```

SUBROUTINE READH (NR,NC,H,HP,HT,HM)
C
C THIS SUBROUTINE READS IN AN INITIAL WATER TABLE ELEVATION OR
C HEAD FOR COMPARING WATER LEVEL CHANGES
C H=INITIAL WATER TABLE ELEVATION(L)
C HT=PRESENT WATER TABLE ELEVATION(L)
C HP=WATER TABLE ELEVATION OR HEAD AT PREVIOUS TIME LEVEL(L)
C HM=HORIZONTAL WATER LEVEL
C LBC=LEFT BOUNDARY CODE
C RBC=RIGHT BOUNDARY CODE
C TBC=TOP BOUNDARY CODE
C BBC=BOTTOM BOUNDARY CODE
C IDENTIFICATION OF BOUNDARY VALUES OF H
C H(I,J) LESS THAN 10000-WATER TABLE ELEVATION( NO BOUNDARY)
C H(I,J) GREATER THAN 10000 BUT LESS THAN 20000- IMPERMEABLE
C H(I,J) GREATER THAN 20000 BUT LESS THAN 30000 - UNDER FLOW
C H(I,J) GREATER THAN 30000 BUT LESS THAN 40000-CONSTANT HEAD
C
C DIMENSION H(NP,NC) , HT(NR,NC) , HP(NR,NC)
C REAL LBC
C READ (5,200) HM,LBC,RBC,TBC,BBC
C DO 100 I = 1,NR
C DO 100 J = 1,NC
C H(I,J) = HM
100 CONTINUE
C DO 110 I = 1,NR
C H(I,1) = LBC + HM
C H(I,NC) = RBC + HM
110 CONTINUE
C DO 120 J = 1,NC
C H(1,J) = TBC + HM
C H(NR,J) = BBC + HM
120 CONTINUE
C DO 130 J = 1,NC
C DO 140 I = 1,NP
C KK = H(I,J)/10000. + 1.0
C GC TO (130,140,150,160), KK
130 HT(I,J) = H(I,J)
C GC TO 170
140 HT(I,J) = H(I,J) - 10000.
C GC TO 170
150 HT(I,J) = H(I,J) - 20000.
C GC TO 170
160 HT(I,J) = H(I,J) - 30000.
170 HP(I,J) = HT(I,J)
180 CONTINUE
C WRITE (6,190)
C CALL MATROP (NR,NC,H)
C RETURN
190 FORMAT (50X, 35HCODED WATER TABLE ELEVATIONS AT T=0)
200 FORMAT (5F10.1)
C END

```

0002
 0003
 0004
 0005
 0006
 0007
 0008
 0009
 0010
 0011
 0012
 0013
 0014
 0015
 0016
 0017
 0018
 0019
 0020
 0021
 0022
 0023
 0024
 0025
 0026
 0027
 0028
 0029
 0030
 0031
 0032
 0033
 0034
 0035
 0036
 0037
 0038
 0039
 0040
 0041
 0042
 0043
 0044
 0045
 0046
 0047
 0048
 0049
 0050
 0051
 0052
 0053
 0054

SUBROUTINE ESATHS

```

SUBROUTINE ESATHS (SLMD,HSQ0,HSQ00,HKQ0,PETA,N)
C
C THIS SUBROUTINE CALCULATES THE EFFECTIVE PERMEABLE HEIGHT AND
C EFFECTIVE SATURATION HEIGHT AS A FUNCTION OF ELEVATION WHEN
C INFILTRATION RATE IS ZERO.
C
C DIMENSION HSQ0(N) , H(2500) , HKQ0(N)
C DO 110 I = 1,N
C H(I) = I
C HDOT = H(I)/HSQ0PH
C IF (HDOT.LE.1.0) GO TO 100
C H(I) = ((SLMD - HDOT) * (1. - SLMD))/(SLMD - 1.0) * HSQ0PH
C HSQ0(I) = ((PETA - HDOT) * (1. - PETA))/(PETA - 1.0) * HSQ0PH
C GO TO 110
100 CONTINUE
C HKQ0(I) = H(I)
C HSQ0(I) = H(I)
110 CONTINUE
C RETURN
C END

```

0002
 0003
 0004
 0005
 0006
 0007
 0008
 0009
 0010
 0011
 0012
 0013
 0014
 0015
 0016
 0017
 0018
 0019
 0020
 0021
 0022
 0023
 0024
 0025
 0026
 0027
 0028
 0029
 0030

SUBROUTINE READPH

```

SUBROUTINE READPH (NR,NC,FK,SY,Z,DX,DY,HF,PHI,D,SLMD,BUBPH,QDOT,Q,
1PETA)
C
C     THIS SUBROUTINE READS AND WRITES THE PHYSICAL DATA DESCRIBING
C     THE SYSTEM.
C     PHI=DRAINABLE POROSITY(DIMENSIONLESS)
C     D=GROUND SURFACE ELEVATION(L)
C     SLMD=PORE SIZE DISTRIBUTION INDEX(DIMENSIONLESS)
C     BUBPH=BUBBLING PRESSURE HEAD(L)
C     QDOT=SCALED FLUX RATE, POSITIVE UPWARDS(DIMENSIONLESS)
C     FFK=UNIFORM HYDRAULIC CONDUCTIVITY(L/T)
C
C     DIMENSION          FK(NR,NC)      , Z(NR,NC)      , DX(NR,NC)      ,
1    DY(NR,NC)      , FF(NR,NC)      , SY(NR,NC)      , Q(NR,NC)
WRITE (6,140)
READ (5,150) PHI,D,SLMD,BUBPH,QDOT,FFK
PETA = 2.0 + (3.0 * SLMD)
WRITE (6,150) PHI,D,SLMD,BUBPH,QDOT,FFK,PETA
DO 100 J = 1,NR
DO 100 K = 1,NC
FK(J,K) = 0.0
SY(J,K) = 0.0
HF(J,K) = 0.0
Z(J,K) = 0.0
Q(J,K) = 0.0
100 CONTINUE
READ (5,200) (DX(I,J),J = 1,NC)
DO 110 I = 2,NR
DO 110 J = 1,NC
DX(I,J) = DX(1,J)
110 CONTINUE
READ (5,200) (DY(I,1),I = 1,NR)
DO 120 J = 2,NC
DO 120 I = 1,NR
DY(I,J) = DY(I,1)
120 CONTINUE
DO 130 J = 1,NR
DO 130 K = 1,NC
FK(J,K) = FFK
130 CONTINUE
READ (5,200) ((Q(I,J),J = 1,NC),I = 1,NR)
WRITE (6,160)
CALL MATROP (NR,NC,DX)
WRITE (6,170)
CALL MATROP (NR,NC,DY)
WRITE (6,180)
CALL MATROP (NR,NC,FK)
WRITE (6,190)
CALL MATROP (NR,NC,Q)
RETURN
C
140 FORMAT (7X, 3HPHI,4X, 1HD,10X, 5HSLMD,5X, 5HBUBPH,6X, 4HQDOT
1,6X, 4HKSAT,7X, 4HPETA)
150 FORMAT (8F10.2)
160 FORMAT (50X, 24HGRID SPACING,X-DIRECTION)
170 FORMAT (50X, 24HGRID SPACING,Y-DIRECTION)
180 FORMAT (50X, 26HHYDRAULIC CONDUCTIVITY MAP)
190 FORMAT (50X, 12HHEAD MAP)
200 FORMAT (8F10.1)
END

```

SUBROUTINE ESATHQ

```

SUBROUTINE ESATHQ (SLMD,PETA,BUBPH,HS,QDOT,N)
C
C THIS SUBROUTINE EVALUATES THE EFFECTIVE SATURATED HEIGHT
C AS A FUNCTION OF ELEVATION WHEN INFILTRATION RATE IS
C GREATER THAN ZERO. INTEGRATIONS ARE PERFORMED BY GAUSSIAN
C QUADRATURE.
C
      DIMENSION      HS(N)      , H(2000)      , WT(12)      ,
1      X(12)
      NUMQPT = 12
      A = 1.
      B = ( - QDOT ) * * ( - 1./PETA )
      C = (B - A)/2.
      D = (B + A)/2.
      WT(1) = .04717533638651
      WT(2) = .10693932599531
      WT(3) = .16007832854334
      WT(4) = .20316742672306
      WT(5) = .23349253653935
      WT(6) = .24914704581340
      WT(7) = .04717533638651
      WT(8) = .10693932599531
      WT(9) = .16007832854334
      WT(10) = .20316742672306
      WT(11) = .23349253653835
      WT(12) = .24914704581340
      X(1) = .98156063424671
      X(2) = .90411725637047
      X(3) = .76990267419430
      X(4) = .58731795428661
      X(5) = .36783149899818
      X(6) = .12523340851146
      X(7) = -.98156063424671
      X(8) = -.90411725637047
      X(9) = -.76990267419430
      X(10) = -.58731795428661
      X(11) = -.36783149899818
      X(12) = -.12523340851146
      ENTGRL = 0.0
      DO 100 I = 1, NUMQPT
        FPDOT = 0.0
        FPDOT = C * X(I) + D
        ENTGRL = ENTGRL + (1./(1 + QDOT * FPDOT * * PETA)) * WT(I) * C
100    CONTINUE
      ZDOT11 = (1./(1. + QDOT)) + ENTGRL
      Z11 = ZDOT11 * BUBPH
      ZDOT1 = 1./(1. + QDOT)
      PSURF = 1.
      DO 170 I = 1, N
        H(I) = I
        HDOT = H(I)/BUBPH
        IF (HDOT.LE.ZDOT11) GO TO 160
        IF (HDOT.GE.ZDOT11) GO TO 140
        CLHS = HDOT - 1./(1. + QDOT)
110    CCNTINUE
        PSURF = PSURF + .0005
        B = PSURF
        C = (B - A)/2.
        D = (B + A)/2.
        RHS = 0.0
        DO 120 K = 1, NUMQPT
          FPDOT = 0.0
          FPDOT = C * X(K) + D
          RHS = RHS + (1./(1. + QDOT * FPDOT * * PETA)) * WT(K) * C
120    CONTINUE
        DIFF = CLHS - RHS
        IF (ABS(DIFF).GT.0.005) GO TO 110
        C = (B - A)/2.
        D = (B + A)/2.
        SINGRL = 0.0
        DO 130 J = 1, NUMQPT
          FPDOT = 0.0
          FPDOT = C * X(J) + D
          SINGRL = SINGRL + (1./((FPDOT * * SLMD) * (1. + QDOT * FPDOT
1          T * * PETA))) * WT(J) * C

```

```

130 CONTINUE
HS(I) = BURPH * (1./ (1. + QDOT) + SINGRL)
GO TO 170
140 A = 1.
Q = (1. - QDOT) * * (1. / PETA)
C = (B - A) / 2.
D = (B + A) / 2.
SINGRL = 0.0
DO 150 L = 1, NUMQPT
FPDOT = 0.0
FPDOT = C * X(L) + D
SINGRL = SINGRL + ((FPDOT * * (1. - SLMD) - (1. - QDOT) * * (S
LMD/PETA)) / (1. + QDOT * FPDOT * * PETA)) * WT(L) * C
150 CONTINUE
HS(I) = BURPH * ((1. - (1. - QDOT) * * (SLMD/PETA)) / (1. + QDOT)
+ (1. - QDOT) * * (SLMD/PETA) * MDOT + SINGRL)
GO TO 170
160 CONTINUE
HS(I) = H(I)
170 CONTINUE
RETURN
END

```

H 0077
H 0078
H 0079
H 0080
H 0081
H 0082
H 0083
H 0084
H 0085
H 0086
H 0087
H 0088
H 0089
H 0090
H 0091
H 0092
H 0093
H 0094
H 0095
H 0096
H 0097
H 0098

SUBROUTINE SPYLD

```

SUBROUTINE SPYLD (HS,HSQ,HT,HP,SY,NC,NR,D,PHI,I5,Q,QDOT,SLMD,PETA) I 0002
1) I 0003
C THIS SUBROUTINE EVALUATES THE SPECIFIC YIELD. I 0004
C I 0005
C I 0006
C DIMENSION HS(2500) , HSQ(2500) , HT(NR,NC) , I 0007
1 HP(NR,NC) , SY(NR,NC) , Q(NR,NC) I 0008
IF (I5.GT.1) GO TO 120 I 0009
DO 110 I = 1,NR I 0010
DO 110 J = 1,NC I 0011
IF (Q(I,J).GT.0.0100) GO TO 100 I 0012
SY(I,J) = PHI I 0013
GO TO 110 I 0014
100 SY(I,J) = PHI * (1. - (1. - QDOT) * * (SLMD/PETA)) I 0015
110 CONTINUE I 0016
RETURN I 0017
120 CONTINUE I 0018
NR1 = NR - 1 I 0019
NC1 = NC - 1 I 0020
DO 130 I = 2,NR1 I 0021
DO 130 J = 2,NC1 I 0022
DO 130 N = 1,2 I 0023
IF (N.EQ.1) HF = HP(I,J) I 0024
IF (N.EQ.2) HF = HT(I,J) I 0025
IF (Q(I,J).EQ.0.000) GO TO 130 I 0026
Z = D - HF I 0027
IZ = Z I 0028
HSA = (HS(IZ + 1) - HS(IZ)) * (Z - IZ) + HS(IZ) I 0029
IF (N.EQ.1) HS1 = HSA I 0030
IF (N.EQ.2) GO TO 140 I 0031
GO TO 130 I 0032
130 CONTINUE I 0033
Z = D - HF I 0034
IZ = Z I 0035
HSA = (HSQ(IZ + 1) - HSQ(IZ)) * (Z - IZ) + HSQ(IZ) I 0036
IF (N.EQ.1) HS1 = HSA I 0037
IF (N.EQ.2) GO TO 140 I 0038
GO TO 130 I 0039
140 CONTINUE I 0040
DIFF = HT(I,J) - HP(I,J) I 0041
IF (DIFF.LT.0.1) GO TO 150 I 0042
HS2 = HSA I 0043
SY(I,J) = PHI * (1.0 + (HS2 - HS1) / (HT(I,J) - HP(I,J))) I 0044
GO TO 130 I 0045
150 CONTINUE I 0046
SY(I,J) = SY(I,J) I 0047
160 CONTINUE I 0048
RETURN I 0049
END I 0050

```

SUBROUTINE EFLOD

C	SUBROUTINE EFLOD (HP,HKQD,HF,NR,NC,D,N)	J 0002
C	THIS SUBROUTINE EVALUATES THE DEPTH AVAILABLE FOR HORIZONTAL FLOW.	J 0003
C	DIMENSION HP(NR,NC) , HKQD(N) , HF(NR,NC)	J 0004
	NR1 = NR - 1	J 0005
	NC1 = NC - 1	J 0006
	DO 100 I = 2,NR1	J 0007
	DO 100 J = 2,NC1	J 0008
	Z = D - HP(I,J)	J 0009
	IZ = Z	J 0010
	EPH = (HKQD(IZ + 1) - HKQD(IZ)) * (Z - IZ) + HKQD(IZ)	J 0011
	HF(I,J) = HP(I,J) + EPH	J 0012
100	CONTINUE	J 0013
	RETURN	J 0014
	END	J 0015

SUBROUTINE MATROP

C	SUBROUTINE MATROP (NOROW,NOCOL,B)	K 0002
C	THIS SUBROUTINE ORGANIZES DATA OR RESULTS INTO A SUITABLE FORM	K 0003
C	FOR PRINTING AND PRINTS.	K 0004
C	DIMENSION B(NOROW,NOCOL)	K 0005
C	NOCOLM = NOCOL	K 0006
	ICNT = 1	K 0007
	NO1 = NOCOLM	K 0008
	IF (NOCOLM.GT.12) NO1 = 12	K 0009
100	NO2 = NOCOLM - 12	K 0010
	WRITE (6,130) (JJ,JJ = ICNT,NO1)	K 0011
	DO 110 I = 1,NOROW	K 0012
110	WRITE (6,140) I,(B(I,J),J = ICNT,NO1)	K 0013
	IF (NO2.LE.0) RETURN	K 0014
	NOCOLM = NOCOLM - 12	K 0015
	ICNT = ICNT + 12	K 0016
	IF (NOCOLM.LE.12) GO TO 120	K 0017
	NO1 = ICNT + 11	K 0018
	GO TO 100	K 0019
120	NO1 = ICNT - 1 + NOCOLM	K 0020
	GO TO 100	K 0021
C		K 0022
C		K 0023
C		K 0024
	130 FORMAT (1H ,//,3X,12(7X,1HX,I2)/)	K 0025
	140 FORMAT (1H ,1HY,I2,12F10.3)	K 0026
	END	K 0027

APPENDIX B

RESULTS FROM EXPERIMENTAL TESTS

Table B-1. Mound Growth Results From Experimental Tests

Media: 2.5 mm Glass Beads

Run: 1

$$H_o = 14.35 \text{ cm}$$

$$\phi_e = 0.35$$

$$D = 32.9 \text{ cm}$$

$$q = 5.05 \text{ cm/min}$$

$$K = 303.96 \text{ cm/min}$$

$$P_b/\rho g = 1.0 \text{ cm}$$

$$\lambda = 7.00$$

Time min	Water Table Height at Distance X From Centerline of Mound (cm)						
	x=15	x=45.5	x=101.5	x=182.5	x=263	x=319.5	x=350
0.5	18.50	18.00	16.00	14.80	14.55	14.50	14.45
2.5	24.60	23.70	22.20	19.50	17.40	16.00	15.30
5.0	27.80	26.60	25.30	22.40	19.50	17.30	16.10

Table B-2, Mound Growth Results From Experimental Tests

Media: 2.5 mm Glass Beads

Run: 2

$$H_o = 14.35 \text{ cm}$$

$$\phi_e = 0.35$$

$$D = 32.9 \text{ cm}$$

$$q = 6.10 \text{ cm/min}$$

$$K = 303.96 \text{ cm/min}$$

$$P_b/\rho g = 1.0 \text{ cm}$$

$$\lambda = 7.00$$

Time min	Water Table Height at Distance X From Centerline of Mound (cm)						
	x=15	x=45.5	x=101.5	x=182.4	x=263	x=319.5	x=350
3.0	27.30	26.50	24.90	21.80	18.90	16.90	15.90
4.5	28.50	28.10	27.00	23.70	20.40	17.80	16.30

Table B-3. Mound Growth Results From Experimental Tests

Media; 2.5 mm Glass Beads

Run: 3

$$H_o = 14.35 \text{ cm}$$

$$\phi_e = 0.35$$

$$D = 32.9 \text{ cm}$$

$$q = 7.34 \text{ cm/min}$$

$$K = 303.96 \text{ cm/min}$$

$$P_b/\rho g = 1.0 \text{ cm}$$

$$\lambda = 7.00$$

Time min	Water Table Height at Distance X From Centerline of Mound (cm)						
	x=15	x=45.5	x=101.5	x=182.5	x=263	x=319.5	x=350
1.5	26.03	24.70	22.70	19.20	16.90	15.70	15.10

Table B-4, Mound Growth Results From Experimental Tests

Media: Ottawa Sand

$$H_o = 6.7 \text{ cm}$$

$$\phi_e = 0.2$$

$$D = 34.5 \text{ cm}$$

$$q = 2.37 \text{ cm/min}$$

$$K = 0.65 \text{ cm/sec}$$

$$P_b/\rho g = 8.8 \text{ cm}$$

$$\lambda = 4.14$$

Time min	Water Table Height at Distance X From Centerline of Mound (cm)						
	x=15	x=45.5	x=101.5	x=182.5	x=263	x=319.5	x=350
0.75	15.50	14.10	10.10	7.50	6.80	6.70	6.70
1.00	17.40	15.90	11.00	8.00	6.90	6.70	6.70
2.25	24.50	22.20	15.30	10.20	8.10	7.20	6.70
2.75	26.30	24.10	17.10	11.00	8.60	7.50	6.90
3.00	27.10	24.90	17.90	11.30	8.80	7.60	7.00